PHILOSOPHICAL TRANSACTIONS OF THE ROYAL SOCIETY B BIOLOGICAL SCIENCES

The Aerodynamics of Hovering Insect Flight. IV. Aerodynamic Mechanisms

C. P. Ellington

Phil. Trans. R. Soc. Lond. B 1984 **305**, 79-113
doi: 10.1098/rstb.1984.0052

Phil. Trans. R. Soc. Lond. B **305**, 79–113 (1984)

Printed in Great Britain

THE AERODYNAMICS OF HOVERING INSECT FLIGHT. IV. AERODYNAMIC MECHANISMS

By C. P. ELLINGTON

Department of Zoology, University of Cambridge, Downing Street, Cambridge CB2 3EJ, U.K.

(*Communicated by Sir James Lighthill, F.R.S.* – *Received* 28 *March* 1983)

[Plate 1]

CONTENTS

Theoretical considerations and available experimental studies are combined for a discussion on the aerodynamic mechanisms of lift generation in hovering animal flight. A comparison of steady-state thin-aerofoil theory with measured lift coefficients reveals that leading edge separation bubbles are likely to be a prominent feature in insect flight. Insect wings show a gradual stall that is characteristic for thin profiles at Reynolds numbers (Re) less than about 10^5. In this type of stall, flow separates

at the sharp leading edge and then re-attaches downstream to the upper wing surface, producing a region of limited separation enclosing a recirculating flow. The resulting leading edge bubble enhances the camber and thickness of the thin profile, improving lift at low *Re*. Some of the results for bird wing profiles indicate that the complications of leading edge bubbles might even be found in the fast forward flight of birds.

It is pointed out that the usual quasi-steady aerodynamic analysis employed for flapping animal flight is incomplete. In addition to the translational motion of the wings, the general quasi-steady formulation should also consider the effects of profile rotation on lift production. Circulatory lift towards the ends of half-strokes should thus be substantially greater than predicted by the usual analysis for hovering, because of the high rates of increase of the angle of attack. Combining this result with the profile flexion observed at the beginning of half-strokes, it is argued that the quasi-steady circulation may be nearly constant during a half-stroke. If this is so, then the mean lift would be proportional to the mean flapping velocity instead of the mean square, as assumed in the usual analysis.

The results from unsteady aerofoil theory provide an insight into the influence of wake vorticity on the bound vorticity of the wings. Vorticity shed into the wake always causes the instantaneous circulation to change more slowly than the quasi-steady assumption would predict: the slow growth of circulation for a wing suddenly set into motion, the Wagner effect, illustrates this process. For animals hovering with a horizontal stroke plane, the growth of circulation on each half-stroke should be even slower because of the influence of vorticity shed on the preceding half-stroke. The maximum circulation actually achieved during a half-stroke should thus be much lower than quasi-steady predictions. In spite of the useful discussions prompted by unsteady theory, it cannot yet be rigorously applied to hovering animal flight, however; modern research in unsteady aerodynamics is attempting to relax various limitations of the theory, but progress to date still lags far behind what is required for an analysis of hovering.

Some hovering animals require more lift than their wings can produce in steady motion. The only conventional unsteady mechanism that can generate enhanced lift is delayed stall. Weis-Fogh proposed a novel mechanism, the 'fling', which creates circulation when the left and right wings come into contact during rotation at the end of the wingbeat. The fling circulation provides lift over the subsequent half-stroke, and can exceed the maximum value for steady motion. Variants on the fling were described in paper III: the 'partial fling', the 'near fling', and the 'peel'. The effectiveness of these mechanisms in creating circulatory lift, and their possible roles in hovering flight are examined in this paper.

Rough estimates indicate that the vorticity shed during isolated wing rotation (without any interference from the image wing) is probably greater than the vorticity bound to the wing during the translational phase of the wingbeat. If this rotational vorticity is shed from the leading edge, it could then be used for circulatory lift as a re-attached leading edge separation bubble over the subsequent half-stroke. Flexion of the wing profile during rotation was observed for all of the insects of paper III, and it is suggested that this 'flex' mechanism could facilitate the required leading edge vortex-shedding. The delayed pronation found for hover-flies using an inclined stroke plane may provide another method of creating circulation by isolated rotation.

These considerations of rotational mechanisms stray far from the usual quasi-steady interpretation of hovering flight. The strong vorticity shed during rotation must have an important, if not dominant, influence on the aerodynamics. The postulated rotational mechanisms simply offer an optimistic interpretation of that influence. With a continuous series ranging from isolated rotation to a complete fling, these mechanisms should also be applicable to most, if not all, hovering animals.

PHILOSOPHICAL TRANSACTIONS OF THE ROYAL SOCIETY B BIOLOGICAL SCIENCES

1. Introduction

The wing kinematics in hovering flight are greatly exaggerated when compared with orthodox wing motions. Indeed, the large amplitude flapping and rotation in the absence of a mean flight velocity make even the most severe examples of the catastrophic flutter of man-made wings seem like gentle callisthenics. What are the aerodynamic mechanisms associated with these motions? Until the appropriate experimental studies are done this question cannot be answered with any certainty, and we must be content with a more speculative discussion for now. This paper offers such a discussion, based on theoretical considerations and the available experimental investigations. I hope that the presentation proves useful for biologists less familiar with the aerodynamic literature, and that the unavoidable simplifications and omissions are not misleading. Further details may be found in many aerodynamic texts, and I have found the following particularly useful: Prandtl & Tietjens (1957), Mises (1959), Duncan *et al.*(1970), Kármán & Burgers (1935), Fung (1969) and Bramwell (1976). Maxworthy (1981) has written an excellent short review of the fluid dynamics of insect flight which, although primarily intended for aerodynamicists, is admirably readable, concise and clear. McCroskey (1982) provides a similar review of modern research on unsteady aerofoils.

A few preliminary notions and definitions are required before beginning in earnest. Except where noted, the discussions apply to *two-dimensional aerofoils*: wings of infinite span, with the same streamline picture for any cross-section perpendicular to the span. It is usually assumed that the three-dimensional flow around a wing of finite span can be derived from the two-dimensional considerations, and this assumption is generally well supported by experiments when the aspect ratio is greater than about 4. Each spanwise element of the finite wing is then treated as a two-dimensional aerofoil with a relative velocity that includes the induced velocities of vortices in the wake. In this manner, three-dimensional effects can be represented by a small change in the local effective angle of attack for a wing element. It should be noted, however, that substantial quantitative and qualitative differences are sometimes found between two- and three-dimensional results (Carpenter 1958; Wagner 1980; McCroskey 1982). Maxworthy's (1979) experimental investigation of Weis-Fogh's (1973) 'fling' mechanism is particularly of interest for hovering insect flight. Maxworthy discovered a strong spanwise transport of vorticity towards the wing tip within the large leading edge bubble created by the fling (§6.1), and suggested that this stabilizes the bubble more that two-dimensional considerations would predict. Whether or not this phenomenon of spanwise transport is more generally applicable to insect flight is unknown at present.

The flight velocity V is negligible in 'hovering', so the velocity of the wing through the undisturbed air is simply given by the flapping velocity U. The *geometric angle of attack* α is therefore measured with respect to the path of the wings, as in paper III. The *effective angle of attack* α_r is measured from the relative velocity vector, and includes the effects of wake vorticity. The angle of attack coresponding to zero lift is denoted by α_0: for symmetrical profiles α_0 is zero, but it is negative for cambered profiles. The *angle of incidence* α' is measured with respect to the zero lift angle, and is equal to $\alpha-\alpha_0$. Similarly, the *effective angle of incidence* α'_r is given by $\alpha_r-\alpha_0$. The angles of attack considered in theoretical aerodynamics are usually small, and are expressed in radians so that small-angle trigonometric approximations can be employed. The experimentalists, however, prefer to measure angles in degrees. Except where noted for some equations, I shall follow the convention of the experimentalists.

PHILOSOPHICAL TRANSACTIONS OF THE ROYAL SOCIETY B BIOLOGICAL SCIENCES

2. Steady motion

2.1. *Circulatory lift*

2.1.1. *Theory*

Consider the simplest aerodynamic situation first: an aerofoil in steady linear motion with velocity U and an angle of attack α well below the stall. If the aerofoil did *not* generate lift, then the average air pressures above and below it would be equal and, by Bernoulli's theorem, the average air velocities along the upper and lower surfaces must be equal as well. The flow pattern corresponding to this is shown in the first term of the pictorial equation of figure 1; the streamlines in front of the section are symmetrical with those behind, and the flow leaves

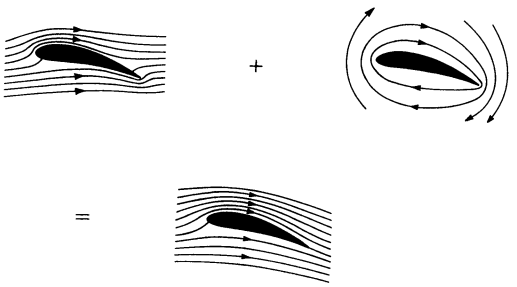

Figure 1. The flow around an aerofoil must leave the trailing edge tangentially to avoid an infinite velocity there. The addition of a unique circulatory flow to that associated with linear motion of the section satisfies this condition.

the wing ahead of the trailing edge at a separation point on the upper surface. This flow pattern is physically impossible, however, because the air velocity becomes infinite at the sharp trailing edge as it moves from the lower to upper surface, producing an infinite shear stress at the trailing edge even when viscosity is negligible. The fluid velocity must remain finite instead, and this occurs only if the flow comes off the trailing edge smoothly and tangential to it: the *Kutta condition*. By adding a circulating flow (the second term of figure 1) to that which would exist if no lift were produced (the first term), the average air velocity is increased over the upper surface and decreased along the lower, moving the rear separation point towards the trailing edge. The circulation Γ around the section is a measure of the velocity difference produced by the circulating flow, which may be thought of as a vortex 'bound' to the section. There is one, and only one, value of Γ that places the separation point at the trailing edge (figure 1) and avoids an infinite velocity there: this unique value is the only one consistent with steady motion of the aerofoil. The velocity difference associated with this circulation must correspond to a pressure difference across the section, and thus accounts for the generation of lift.

The lift per unit span due to circulation around an aerofoil in steady motion is given by the Kutta–Joukowski theorem as

$$L' = \rho U \Gamma, \tag{1}$$

where ρ is the density of air (or other fluid). The unique value of the circulation satisfying the Kutta condition for linear motion, or *translation*, is

$$\Gamma_t = \pi c U \sin \alpha' \approx \pi c U \alpha', \tag{2}$$

and when this is substituted in equation (1) it determines the lift for a given velocity, angle of incidence and chord c. (The approximation is valid for small values of α', which must be expressed in radians.) The expression for lift in terms of the lift coefficient C_L,

$$L' = \tfrac{1}{2}\rho c U^2 C_L, \tag{3}$$

may be combined with equations (1) and (2) to derive

$$C_L = 2\pi \sin \alpha' \approx 2\pi\alpha'. \tag{4}$$

This theoretical expression applies to all thin sections in *translation*: the profile shape only affects the zero lift angle α_0, which is incorporated in α'.

The resultant circulatory lift force acts at the one-quarter chord point according to thin aerofoil theory, and this is true for unsteady motion as well as the steady case. For many purposes, therefore, we may regard the bound vortex as concentrated at a distance $\frac{1}{4}c$ behind the leading edge. It must be understood that the 'bound vortex' is only a useful theoretical construct, though, and not a physical reality. The theory additionally shows that the angle of incidence should be measured at the three-quarters chord point: this result is also valid in general and is required for some special cases of wing motion, such as rotation about a spanwise axis.

2.1.2. *Experiment*

Experimental results for conventional profiles at high Reynolds numbers (*Re* greater than about 10^5) generally confirm equations (2) and (4) at angles of incidence below stall, except for the fact that observed values of Γ_t and C_L are about 90 % of the predicted ones (Fung 1969). Very few studies have been made at *Re* less than 10^5, however, and investigations on real or model animal wings are even more scarce. The available results for insect wings, which are most relevant to this study, were briefly discussed in paper I and are presented in figure 2. C_L is plotted against the drag coefficient C_D in the usual manner of polar diagrams, with the angle of attack indicated on the curve. These measurements were made on real wings of finite span, instead of models giving approximately two-dimensional flow, and cannot be compared directly with the theory without correcting them for the downwash of trailing vortices (paper V). The downwash depends on the circulation distribution along the span, that is the circulation around each wing element, and since this is unknown an accurate correction cannot be made. Furthermore, the measurements for the locust forewing (Jensen 1956) were made in a wind tunnel that produced a velocity gradient from wing base to tip, simulating the wing velocity in flapping flight; this may alter the circulation distribution and downwash pattern considerably from that obtained in an orthodox wind tunnel, as used for the *Drosophila* (Vogel 1967) and *Tipula* (Nachtigall 1977) wings. Nachtigall (1981) has measured the lift of model locust wings placed in the parallel airstream of a conventional tunnel, and also rotated like a propeller in still air. With use of his results for a Reynolds number of 1100, an approximate comparison can therefore be drawn with Jensen's experiments at $Re = 2000$. Both authors measured polars for a *flat* profile of the forewing, which is found during most of the downstroke, and a *cambered* profile, which results from depression of the vannal region as a flap late in the downstroke. They also present results for the Z profile of the early upstroke; this profile seems peculiar to locusts in fast forward flight, however, and will not be discussed here.

The slope of the lift–incidence curve, $dC_L/d\alpha'$, has a theoretical value of 2π for two-dimensional

PHILOSOPHICAL TRANSACTIONS OF THE ROYAL SOCIETY B BIOLOGICAL SCIENCES

aerofoils at small angles of incidence. This value decreases with the aspect ratio for wings of finite span, and is also dependent on the circulation distribution. At small α', $dC_L/d\alpha'$ is approximately 2.2 for the flat *Drosophila* wing, 3.6 for the cambered one, 4.0 for the *Tipula* wing, 4.0 and 5.0 for Jensen's flat and cambered locust forewings, and 5.3 for Nachtigall's (1981) model locust forewings measured in a conventional wind tunnel. These results are generally comparable with two-dimensional theory if crudely corrected for downwash, but a firmer conclusion cannot be justified because of the assumptions necessarily invoked. An interesting point is that $dC_L/d\alpha'$ increases with camber for *Drosophila* and Jensen's locust wings, although the theory predicts that this should not happen.

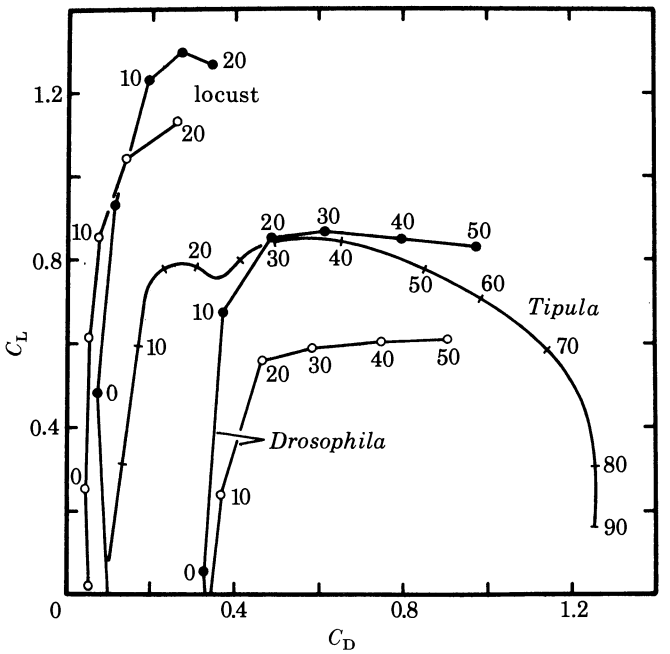

FIGURE 2. Polar diagrams of insect wings. The angle of attack is given in degrees along each curve. Reynolds numbers are 2000 for the locust *Schistocerca gregaria* forewing (Jensen 1956); 1500 for the *Tipula oleracea* wing (Nachtigall 1977); and 200 for the *Drosophila virilis* wing (Vogel 1967). Open circles are for flat wings of *Drosophila* and *Schistocerca*, closed circles are for cambered wings.

Conventional wings never reach the maximum theoretical value of C_L ($= 2\pi$) because they *stall* long before α' reaches 90°: the flow breaks away from the upper surface near the leading edge, producing a thick wake with high drag and destroying the lifting ability of the wing. As α' increases beyond small angles, C_L rises more slowly until a *maximum lift coefficient* $C_{L,\,max}$ is reached, and the lift then decays more or less sharply as the wing stalls with further increases of α'. It should be noted that $C_{L,\,max}$ is not affected by the aspect ratio, which only alters the angle of incidence at which $C_{L,\,max}$ is reached. Values of $C_{L,\,max}$ for the insect wings are 0.6 and 0.8 for the flat and cambered *Drosophila* wings ($Re = 200$), which compares very well with the results of Thom & Swart (1940) for a flat-bottomed aerofoil at similar low Re, and 0.85 for the *Tipula* wing ($Re = 1500$). Values for the locust forewing are substantially higher in general, even though the Reynolds numbers are comparable with the *Tipula* wing: Jensen's values are 1.1 and 1.3 for the flat and cambered profiles, whereas Nachtigall's model wings gave 0.75 and 1.25 respectively in a parallel airstream. Lift coefficients were not presented for Nachtigall's models rotating like propellers, but the maximum lift force was about the same

for both profiles. This is an anomalous result, implying equal values of $C_{L,max}$ instead of an increased value with camber, as is normally found.

The most interesting feature of the insect wings is the absence of the *abrupt* stall commonly found for conventional, thick profiles at high *Re*. The wings of *Drosophila* and *Tipula* show a very gradual stall, giving values of C_L near $C_{L,max}$ at angles of attack up to 50°. Jensen's experiments did not extend to such high α, but Nachtigall's locust models clearly exhibited a 'mushy' stall like the *Tipula* wing.

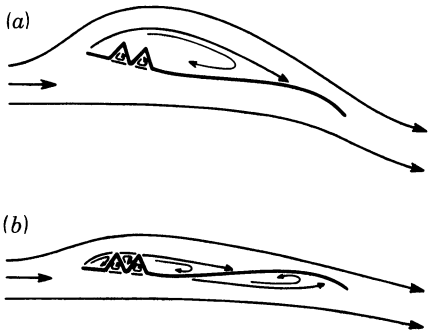

FIGURE 3. (*a*) The large leading edge separation bubble, enclosing a recirculating flow, for a model dragonfly profile at large incidences. (*b*) Small bubbles filling the corrugations are clearly seen at low incidences. The envelope around these bubbles forms a smooth effective profile for the corrugated insect wing. Adapted from Newman *et al.* (1977).

A gradual stall is characteristic for thin profiles at *Re* less than about 10^5, and this 'thin-aerofoil' stall is one of the three basic types discussed by McCullough & Gault (1951), Crabtree (1959) and Tani (1964). The boundary layer tends to remain laminar at these Reynolds numbers, but the sharp deceleration as the flow rounds the thin leading edge causes the laminar boundary layer to break away from the upper wing surface. The separated layer mixes with the surrounding air, thus gaining enough kinetic energy to become turbulent. The energized layer then re-attaches to the downstream upper wing surface, forming a leading edge *separation bubble* (figure 3*a*). In contrast to the well separated flow normally associated with stalling or the wake behind a bluff body, the bubble is a region of limited separation enclosing a recirculating flow. The re-attachment point moves progressively rearward with increasing incidence, producing a long bubble that may eventually extend beyond the trailing edge. Formation of the long bubble is often indicated by a kink in the values of C_L, like the one around α equal to 20–25° for the *Tipula* wing. The separation bubble clings tenaciously to the profile, providing an envelope around which the oncoming air flows. Small bubbles have also been observed trapped in the valleys between veins on insect wing models (Rees 1975; Newman *et al.* 1977); as shown in figure 3, the envelope around these bubbles results in a smooth *effective profile* for the corrugated insect wing.

A thorough investigation of stalling behaviour is lacking for *Re* less than about 10^4, which is the range applicable to insect flight. It is doubtful whether one can speak of transition to turbulence in the separated laminar boundary layer at these low *Re*, but leading edge separation bubbles are clearly evident around thin wing models at *Re* of 200 (Vogel 1967) and even 32 (Maxworthy 1979), where turbulence cannot occur. Bubble re-attachment is promoted at these very low *Re* by an enhanced diffusion of vorticity in the separated laminar layer, which

is analogous to the increased diffusion provided by transition to turbulence at higher *Re* (Lighthill 1973). Below some critical *Re* the bubble thus re-attaches in a laminar form; the locust and *Tipula* wings are also likely to fall into this laminar re-attachment class, with *Re* of 2000 and 1500 respectively. Regardless of the re-attachment mechanism, we should expect separation bubbles to govern the stalling behaviour of insect wings, and those bird and bat wings with a thin leading edge. The importance of a sharp leading edge in assuring separation of the laminar boundary layer, and of the resulting separation bubble in determining the aerodynamic characteristics of the profile, is demonstrated by Nachtigall's (1977) results: the polar of a flat model of the *Tipula* wing was very similar to the real wing, implying that corrugations and surface details have little effect on the wing performance at that *Re*. Vogel (1967) found some differences between real and model wings at the lower *Re* of 200, however; more experimental work is obviously required in this fascinating *Re* range.

Although not appropriate for this study, lift and drag coefficients have been measured for wing models in *two-dimensional* flow at higher *Re*: a model dragonfly profile at *Re* of 12000–25000 and a larger model at 25000–35000 (Newman *et al.* 1977), and three profiles from a pigeon wing at *Re* of 27000, 54000 and 80000 (Nachtigall 1979*a*). For the dragonfly model in the lower *Re* range, $dC_L/d\alpha'$ at small angles of incidence is about 5 and is again comparable with theory. The dragonfly and pigeon profiles show a different behaviour at *Re* greater than 25000, though; $dC_L/d\alpha'$ is about 11 and 14 respectively, around twice the theoretical value. Newman *et al.* explain their result by changes in the effective profile produced by separation bubbles, an idea that is supported by their flow visualization studies. Figure 3*b* shows the bubbles around the dragonfly section at low values of α', and the large posterior bubble on the lower surface should be noted in particular. As the angle of incidence increases (figure 3*a*), this bubble disappears and a leading edge bubble grows along the upper surfaces, increasing the camber of the effective profile with α'. The theoretical value of 2π for $dC_L/d\alpha'$ applies to a fixed profile, and is *not* valid for the variable profile provided by the separation bubbles. Although this phenomenon is not apparent in the results at *Re* less than 25000, where values of $dC_L/d\alpha'$ are close to theory, it may be involved in the differences between flat and cambered *Drosophila* and locust wings at much lower *Re*.

The effect of separation bubbles on $dC_L/d\alpha'$ is further complicated by the results of Withers (1981) for detached bird wings at *Re* from 10000 to 50000. His values for $dC_L/d\alpha'$ ranged from 2.9 to 5.7, and were always less that 2π. This might imply that the effective profile for real, finite span wings is not altered by separation bubbles over that *Re* interval, but the absence of an abrupt stall at large angles of attack indicates that such bubbles were present; indeed, his results for swift and petrel wings show tell-tale kinks in the values of C_L, although not as pronounced as those for the two thinner profiles from a pigeon wing in Nachtigall's (1979*a*) two-dimensional study.

When compared with the experimental data, the theory of thin aerofoils may seem of little use in an analysis of animal flight, even for cases of steady motion such as gliding flight. At high *Re*, the circulation satisfying the Kutta condition agrees well with experiment because the flow follows the profile smoothly. Separation bubbles may be present at *Re* less than 10^5, however, and the effective profile must be taken around them. Leading edge bubbles should prove particularly useful, giving wings an enhanced camber and thickness and thus improving lift at low *Re*. The Kutta condition still applies, but the effective profile may change with angle of attack: this alters the zero lift angle α_0, and so there is no longer a linear correspondence

PHILOSOPHICAL TRANSACTIONS OF THE ROYAL SOCIETY B BIOLOGICAL SCIENCES

between α' and α. The effective profile cannot be predicted by theory, and so C_L must be measured experimentally. The circulation around the wing can then be calculated by using equation (1) from the Kutta–Joukowski theorem and the definition of C_L in equation (3):

$$\Gamma = \tfrac{1}{2}cUC_L. \tag{5}$$

Nachtigall's (1979*a*) results demonstrate that $dC_L/d\alpha'$ is much greater than 2π for pigeon profiles at *Re* up to 80000: thus the complications of separation bubbles may apply even to the fast forward flight of many birds and bats. The value of $dC_L/d\alpha'$ in theories of fast flapping flight based on equation (4) (see, for example: Holst & Küchemann 1941; Lighthill 1977; Phlips *et al.* 1981) may therefore need to be modified after future experimental work investigates the differences between the results of Nachtigall (1979*a*) and Withers (1981). Indeed, a great deal of experimental work is required before we can make satisfactory empirical adjustments to the conceptual and theoretical framework of thin aerofoil theory.

2.2. *Drag*

The lift on an aerofoil is ultimately attributable to viscosity. The purpose of the Kutta condition, which determines the amount of circulatory lift produced, is to ensure that the viscous shearing stresses at the trailing edge do not become infinitely large. In a fluid with zero viscosity, an inviscid fluid, this problem would not arise and the streamlines would be those for zero lift in figure 1. The tribute levied for this useful phenomenon of lift is the accompanying drag force, an unavoidable consequence of viscosity.

There are two components of drag for a two-dimensional aerofoil. The first is *skin friction*, which is a direct result of the viscous shearing stresses in the boundary layer and can be minimized by making the surface of the section very smooth. The boundary layer loses energy because of these stresses, and it separates from the aerofoil before reaching the trailing edge. Although some separated layers may re-attach to the profile, forming separation bubbles, the boundary layer still cannot quite reach the trailing edge. The *wake* produced by this final separation is a region of low pressure, giving rise to the second component of drag, *pressure drag*. This component is small, of course, for thin sections parallel to the flow. The sum of these two components is usually called the profile drag D'_{pro}, and the profile drag coefficient $C_{\mathrm{D,\,pro}}$ is defined by

$$D'_{\mathrm{pro}} = \tfrac{1}{2}\rho cU^2 C_{\mathrm{D,\,pro}}, \tag{6}$$

where the prime denotes a force per unit span as before. For most sections the profile drag varies but little for angles of incidence well below stall, but the pressure drag component increases at larger angles: a plot of $C_{\mathrm{D,\,pro}}$ against α' often shows a relation that is approximately parabolic.

The profile drag is also influenced by the Reynolds number and the state of the boundary layer. That part of $C_{\mathrm{D,\,pro}}$ due to skin friction is less for laminar boundary layers than turbulent ones, where the velocity gradient is steeper, and it decreases with *Re* for both cases. For a smooth flat plate parallel to the flow a gradual transition from laminar to turbulent boundary layer occurs around *Re* equal to 3×10^5, but this critical *Re* is markedly lowered by surface roughness. The kinetic energy of a turbulent boundary layer is relatively higher, which delays the final separation and reduces the pressure drag contribution to the profile drag coefficient. This effect is usually greater than the increase in skin friction, resulting in a drop of $C_{\mathrm{D,\,pro}}$ at transition to a turbulent boundary layer.

PHILOSOPHICAL TRANSACTIONS OF THE ROYAL SOCIETY B BIOLOGICAL SCIENCES

Although the profile drag coefficient can be calculated in some cases, it must be experimentally determined in general. This is especially true for the complex flows associated with separation bubbles. $C_{D,pro}$ should be measured on models that approximate the two-dimensional flow around aerofoils of infinite span, by using high aspect ratios or endplates on the model. If this is not done, a third drag component appears, the *induced drag*. This drag arises from a tilt of the relative velocity vector by the downwash; hence it is related to the lift of the finite span wings (paper V). The induced drag coefficient is proportional to C_L^2, and so its contribution to the polar diagram consists of a parabola lying on its side and opening to the right. The induced drag is a function of aspect ratio and circulation distribution: it can be calculated if these are known, and then subtracted from the total drag coefficient to obtain $C_{D,pro}$. The importance of two-dimensional results cannot be over-emphasized for flapping flight; they are essential to the development of any *generalized* analytical model. Many aerodynamic parameters depend on the circulation distribution, which will vary under different conditions: angles of attack along the span, the wing shape, the ratio of flapping to flight velocity, and the inclination of the stroke plane among others. By using two-dimensional data in vortex theories, such as the one presented in paper V, the induced drag and other three-dimensional effects can be calculated for these different conditions from a single set of experimental results.

The polar diagrams in figure 2 were obtained from real wings, and so a contribution from induced drag appears in the drag coefficient. This will be negligible when lift is small, however, and we may use the minimum value of the drag coefficient $C_{D,min}$ as an estimate of the minimum profile drag coefficient for the wings: $C_{D,min}$ is about 0.34 for the flat and cambered *Drosophila* wings, 0.10 for the *Tipula* wing and Nachtigall's flat and cambered locust wing models, and 0.045 and 0.072 for Jensen's flat and cambered locust wings. At these low Re the boundary layer should be laminar, and skin friction will form a large part of the profile drag. Hence it is informative to compare these values with the drag coefficient for a smooth flat plate at an angle of attack equal to zero, because the drag is entirely due to skin friction for this case and is a theoretical minimum. The well known solution of the laminar boundary layer equations by Blasius gives the drag coefficient due to skin friction $C_{D,f}$ as

$$C_{D,f} = 2.66/Re^{\frac{1}{2}}, \tag{7}$$

for perfect laminar flow over the smooth plate. The Reynolds number is based on the profile chord:

$$Re = cU/\nu, \tag{8}$$

where the kinematic viscosity ν is 1.46×10^{-5} m^{-2} s^{-1} for air at 15 °C and normal atmospheric pressure. Although $C_{D,min}$ is greater than $C_{D,f}$ in practice, because of pressure drag and irregularities in the boundary layer flow, it is still commonly found that $C_{D,min}$ is inversely proportional to $Re^{\frac{1}{2}}$ over a large range. Vogel (1967) presents data on the *Drosophila* wings for four values of Re, from which the approximate relation can be derived:

$$C_{D,min} = 4.8/Re^{\frac{1}{2}}. \tag{9}$$

Thus the minimum profile drag is nearly twice the skin friction of a flat plate parallel to the flow. Equation (9) is also in good agreement with the results of Thom & Swart (1940) for a flat-bottomed profile at low Re, and it predicts $C_{D,min}$ for the *Tipula* wing quite well (0.12 compared with the measured 0.10). The value predicted by equation (9) for the locust wing is 0.11, which is considerably more than Jensen's measurements but comparable with

Nachtigall's model experiments. It should be noted, however, that $C_{D,f}$ for a Reynolds number of 2000 is 0.059. The minimum drag for the flat locust forewing, consisting of skin friction and pressure drag, is *less* than the skin friction drag of a smooth flat plate. This is not theoretically possible, so Jensen's drag values for the flat locust forewing should be rejected, and probably the cambered wing as well. Although equation (9) gives a satisfactory fit to the meagre data on insect wings over *Re* from around 100 to several thousand, except for Jensen's values, it does not agree with the results of Newman *et al.* (1977) on dragonfly profiles at *Re* greater than 10^4.

The induced drag will be nearly constant over the broad plateau of C_L for the *Drosophila* and *Tipula* wings, so the increase of C_D with α in this region represents an enhanced profile drag at approximately the same C_L. The wings of hovering insects operate at large geometrical angles of attack during much of each half-stroke, typically around 35° (paper III), which places them near the middle of the plateau. The comparison is not exact because the effective angle of attack, which depends on the circulation distribution, will be somewhat different for the two cases. Nonetheless, the wings are still operating in an unfavourable region of the polar diagram for *steady motion*: an unnecessarily large profile drag would be incurred for the lift generated.

3. The quasi-steady assumption

The simplest analysis for a wing in unsteady motion is a direct extension of the preceding section and involves the quasi-steady assumption: the instantaneous forces on an aerofoil in unsteady motion are assumed to be those corresponding to steady motion at the same instantaneous velocity and attitude. Thus U and α' may change with time, but their past history is of no importance to the present. The instantaneous lift experienced by a section is then solely dependent on the circulation satisfying the Kutta condition for motion at that moment.

The quasi-steady analysis does not consist of a straightforward application of the theory and experiments for steady linear motion, although all animal flight studies (including my own) have previously done so. In addition to translation, the general formulation of the quasi-steady approximation also includes *rotation* of the section with angular velocity ω ($= \mathrm{d}\alpha/\mathrm{d}t$) about some axis located a distance x_0 behind the leading edge (Fung 1969). This rotation will alter the airflow around the section, and the Kutta condition must be applied to the *net* motion resulting from translation and rotation. The required circulation Γ_q for the quasi-steady case is simply the sum of that satisfying the translational motion, Γ_t, and that satisfying rotation, Γ_r. Application of the Kutta condition to rotational motion yields

$$\Gamma_r = \pi\omega c^2(\tfrac{3}{4}-\hat{x}_0), \tag{10}$$

where $\hat{x}_0$ is equal to x_0/c and ω is measured in radians per second. It was shown in paper III that the axis of wing rotation lies somewhere in the anterior half of the wing, so $\hat{x}_0$ is less than $\frac{1}{2}$ and is likely to be about $\frac{1}{4}$. The total quasi-steady circulation Γ_q around the section is given by

$$\Gamma_q = \Gamma_t + \Gamma_r = \pi cU\sin\alpha' + \pi\omega c^2(\tfrac{3}{4}-\hat{x}_0) \approx \pi cU[\alpha' + (\omega c/U)\,(\tfrac{3}{4}-\hat{x}_0)]. \tag{11}$$

The expression in square brackets represents the angle of incidence at the three-quarters chord point due to translation and to rotation about the axis $\hat{x}_0$. The ratio $\omega c/U$ was introduced in paper III, and may be interpreted as the angle through which the wing rotates during one chord of translation.

Equation (11) highlights the importance of rotation in a quasi-steady analysis of hovering

animal flight. The flapping velocity U varies linearly along the wing, while ω retains the same value, so $\omega c/U$ must be inversely proportional to the radial position of a wing element. The effects of very small rotations are thus magnified for the basal wing area, where the circulation due to rotation may be comparable with that from translation for much of the cycle. Rotation and translation are out of phase during the wingbeat, so $\omega c/U$ becomes infinitely large for the entire wing at either end of the cycle and must dominate the quasi-steady analysis there. The circulation due to translation, however, will be more important for distal wing areas in the middle of each half-stroke.

The total quasi-steady circulation around a wing element may remain roughly constant for much of each half-stroke. The rotational circulation Γ_r increases at the end of a half-stroke because ω is positive, offsetting the reduction in Γ_t that must occur as the flapping velocity drops to zero; it will be shown in §6.4 that this compensation might result in a nearly constant value of Γ_q for much of the wing from the middle to the end of each half-stroke. At the beginning of each half-stroke ω is negative, though, and would reduce the circulation if the wing rotated uniformly. In paper III it was found that the wing *flexes* across the chord at this time: the anterior half of the wing completes rotation while the flapping velocity is still very small, producing a cambered profile as the wing accelerates into the half-stroke. Most of the camber then disappears as the flapping velocity increases and the posterior wing area completes rotation. The effect of this *differential* rotation may be interpreted as a profile with camber inversely related to the translational velocity. Camber increases α' for a profile by effectively reducing α_0, and so increases the translational circulation Γ_t. Thus the profile changes at the beginning of a half-stroke may also enhance Γ_q at low flapping velocities, but this cannot be assessed quantitatively without more extensive data.

The quasi-steady lift L'_q on a wing in translation and rotation is equal to $\rho U\Gamma_q$, where the circulation is given by equation (11). *If the quasi-steady circulation is roughly constant during a half-stroke, then the mean lift must be proportional to the mean flapping velocity* $\bar{U}$. The previous quasi-steady analyses of hovering discussed in paper I did not consider the effects of rotation, and assumed that the mean lift was proportional to the *mean square* of the flapping velocity. The complete expression for the quasi-steady lift coefficient is

$$C_L = 2\pi[\sin\alpha' + (\omega c/U)\,(\tfrac{3}{4}-\hat{x}_0)] \approx 2\pi[\alpha' + (\omega c/U)\,(\tfrac{3}{4}-\hat{x}_0)]. \qquad (12)$$

Whenever C_L is dominated by the $\omega c/U$ term, or else α' is inversely proportional to U, then the section lift will be proportional to the *first* power of velocity.

If the quasi-steady circulation is nearly constant, as suggested by the discussion above, then C_L must be proportional to $1/U$ during the half-stroke. The implications of this are twofold: (i) the assumption of a constant C_L in solving for a mean lift coefficient by the usual quasi-steady analysis is invalidated, and (ii) C_L must reach values larger than the maximum experimental $C_{L,\max}$ when the flapping velocity is small. Although the second point appears to contradict experiments, this does not really provide an excuse for dismissing the theoretical considerations: values of $C_{L,\max}$ measured under steady translation cannot be applied directly to the conditions of rotation and translation. I shall return to this point after other arguments and related experiments are presented in later sections.

PHILOSOPHICAL TRANSACTIONS OF THE ROYAL SOCIETY B BIOLOGICAL SCIENCES

4. Unsteady aerofoil theory

4.1. *Wake vorticity*

The Kutta condition is one of the foundation stones of aerodynamic analyses, and the circulation around a section in unsteady motion is assumed to adjust instantaneously so that the trailing edge velocity is always finite. The other condition that must be satisfied is a consequence of *Kelvin's circulation theorem*; whenever the strength of the bound vortex changes by some amount $\mathrm{d}\Gamma$, an equal but opposite amount of circulation $-\mathrm{d}\Gamma$ must be shed into the wake from the trailing edge. Thus the algebraic sum of circulations about the section and all shed vortices in the wake is zero. This is shown in figure 4*a* for a section that was suddenly set in steady linear motion: the circulation Γ about the aerofoil is exactly balanced by the 'starting vortex' of strength $-\Gamma$ left behind. The air between the two vortices acquires a downward velocity and momentum because of them, and the lift on the aerofoil can be interpreted as the reaction to the time rate of change of this momentum: as the distance between the bound and starting vortices increases, more air is given a downward momentum.

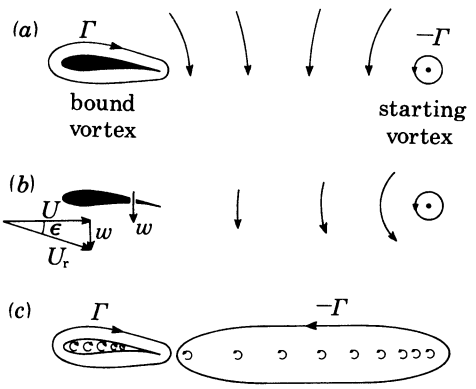

Figure 4. (*a*) The starting vortex balances the circulation of the bound vortex, and the air between is given downward momentum. (*b*) The starting vortex induces a downwash velocity w at the $\frac{3}{4}$ chord point, changing the direction of the relative velocity. (*c*) Representation of bound and shed vorticity as continuous distributions instead of discrete vortices.

The rotational air motion associated with shed vortices also influences the flow around the section, producing a change in the effective angle of incidence α'_{r} in the same manner as the trailing vortices for a wing of finite span. The flow around a single vortex follows circular streamlines, and the velocity w of this vortex motion is inversely proportional to the radius r of the streamlines:

$$w = \Gamma/2\pi r, \tag{13}$$

where Γ is the strength of the vortex. (This equation does not hold for very small values of r because of a viscous 'core' that tends to rotate uniformly, avoiding an infinite velocity at $r = 0$.) Thus the starting vortex of strength $-\Gamma$ will induce a downwash velocity at the aerofoil $w = -\Gamma/2\pi l$, as in figure 4*b*, where l is the distance between the starting vortex and the three-quarters chord point. This changes the velocity 'seen' by the section from U to the relative velocity U_{r}. It also decreases the effective angle of incidence α'_{r} from α' by a small amount ϵ, where $\epsilon = \tan^{-1}(w/U) \approx w/U$. By combining this result with equation (2), which gives the Kutta circulation for translation,

$$\epsilon \approx -\tfrac{1}{2}\alpha' c/l, \tag{14}$$

and the effective angle of incidence can be written as

$$\alpha'_{\mathrm{r}} = \alpha' + \epsilon \approx \alpha'(1 - \tfrac{1}{2}c/l). \tag{15}$$

The downwash of the starting vortex reduces α'_{r} when the aerofoil is close to it, but the effect falls off inversely with l.

The instantaneous circulation Γ around the section must satisfy the Kutta condition for the induced velocity of wake vorticity as well as the quasi-steady motion. The circulation corresponding to α'_{r} is

$$\left.\begin{aligned} \Gamma &\approx \pi c U \alpha'_{\mathrm{r}} = \pi c U \alpha' + \pi c U \epsilon, \\ \Gamma &= \Gamma_{\mathrm{q}} + \Gamma_{\mathrm{i}} \approx \Gamma_{\mathrm{q}}(1 - \tfrac{1}{2}c/l); \end{aligned}\right\} \tag{16}$$

Γ may therefore be regarded as the sum of the quasi-steady circulation Γ_{q} and the circulation induced by the wake vorticity Γ_{i}. The influence of the starting vortex reduces the net circulation Γ required for the Kutta condition, though this effect is again inversely proportional to l, and Γ asymptotically approaches the quasi-steady value as the aerofoil moves along the flight path. Jensen (1956) used this type of analysis to show that the effect of the starting vortex is negligible in locust flight because of the large values of l, and concluded that a quasi-steady approximation was valid for that case.

The amount of vorticity shed into the wake from the trailing edge balances the change in Γ and is equal to $-(\mathrm{d}\Gamma/\mathrm{d}l)\,\mathrm{d}l$: this is proportional to l^{-2}, so the section must deposit progressively weaker vorticity in the wake. Instead of the discrete starting vortex considered in figure 4*a*, *b*, a better model of the wake would be a continuous distribution of vorticity – a *vortex sheet* – as shown in figure 4*c*. The downwash angle ϵ and the induced circulation Γ_{i} were calculated above assuming that all of the wake vorticity is located at the starting point. This is a fair approximation after the section has moved several chord lengths, because most of the wake vorticity is concentrated near that point. For a proper analysis, however, the spatial distribution of wake vorticity must be taken into account. Similarly, the bound vortex is but a crude representation of the vorticity distributed along the upper and lower surfaces of the section, and the aerofoil may be replaced by another vortex sheet.

This simple analysis of the starting vortex has led us to unsteady aerofoil theory through a side door, avoiding the trauma of a more brusque introduction. A complete description of the flow around a section must include the quasi-steady motion (U, α' and ω) and the induced velocity of all wake vorticity. The instantaneous circulation Γ for the aerofoil may be regarded as the sum of two terms: (i) the circulation satisfying the Kutta condition for the quasi-steady motion, Γ_{q}, and (ii) that satisfying the condition for the induced velocity of the wake vorticity, Γ_{i}. As the circulation around the section changes in sympathy with the demands of Γ_{q} and Γ_{i}, new vorticity is shed into the wake from the trailing edge. The key process in unsteady aerofoil theory is solving for a vortex system, representing the continuous distribution of bound and wake vorticity, that is consistent with these general requirements for an aerofoil executing some arbitrary motion. In principle, unsteady theory simply adds the effects of wake induced circulation to the quasi-steady analysis: this process is illustrated by the crude analysis of the starting vortex above, which is approximately correct when the vortex is at least one chord length behind the trailing edge. In practice, however, unsteady theory is rife with rather unpleasant integral equations.

The unsteady effects associated with wake vorticity depend on the distance between the

section and a particular vortex in the wake. Some non-dimensional measure of distance along the flight path is convenient, and λ will denote the distance in chord lengths from the trailing edge to its initial position. The *total* number of chord lengths travelled by a section during a half-stroke will be especially important, and it is given by

$$\Lambda = \Phi r/c, \tag{17}$$

where Φ is the stroke angle in radians and r is the distance from the wing base. Λ will vary along the wing, of course, so a mean value $\overline{\Lambda}$ is derived for the mean distance travelled by the mean chord:

$$\overline{\Lambda} = \tfrac{1}{2}\Phi R/\bar{c} = \tfrac{1}{4}\Phi \mathcal{R}, \tag{18}$$

where R is the wing length and $\mathcal{R}$ is the aspect ratio, equal to the wing span divided by the mean chord. (The reader should note that Weis-Fogh (1973) used λ for the total distance in chords travelled by the wing element at $\hat{r}_2(S)$, which was defined in paper II. Although this reflects the prejudice of his quasi-steady analysis, my choice of definitions is no less arbitrary: $\overline{\Lambda}$ is simply easier to calculate.)

TABLE 1. VALUES OF $\overline{\Lambda}$ FOR SOME HOVERING ANIMALS

$\overline{\Lambda}$ is the mean distance travelled by the wing during a half-stroke, divided by the mean chord. The identification code ID and figure number, if necessary, are given for those insects from paper III. Other references: (1) R. Å. Norberg (1975), (2) U. M. Norberg (1975), (3) U. M. Norberg (1976), (4) Weis-Fogh (1972).

	$\overline{\Lambda}$	reference
inclined stroke plane		
Aeschna juncea	2.5	(1)
Episyrphus balteatus	2.3	(HF08, figure 10, paper 3)
E. balteatus	2.4	(HF08, figure 11, paper 3)
Ficedula hypoleuca	1.9	(2)
Plecotus auritus	3.2	(3)
horizontal stroke plane		
Amazilia fimbriata fluviatilis	3.6	(4)
Apis mellifera	3.8	(HB01)
Bombus hortorum	3.4	(BB04)
B. lucorum	3.8	(BB08)
E. balteatus	3.4	(HF07)
Eristalis tenax	3.3	(DF01, figure 12, paper 3)
E. tenax	3.2	(DF01, figure 13, paper 3)
Coccinella 7-punctata	5.4	(LB04)
Tipula obsoleta	5.8	(CF02)
Tipula paludosa	5.9	(CF04)

Values of $\overline{\Lambda}$ are presented in table 1 for the insects considered in paper III and other hovering animals taken from the literature. The values are very similar to Weis-Fogh's, and they fall into three distinct groups. $\overline{\Lambda}$ is lowest for the animals that hover with an inclined stroke plane, and their wings move only 2 or 3 chord lengths during each half-stroke. The remaining animals use a horizontal stroke plane, and appear to be divided into two groups. $\overline{\Lambda}$ is between 3 and 4 for the drone-fly *Eristalis*, the honey bee *Apis*, the bumble bees *Bombus*, and the hummingbird *Amazilia*; it is particularly interesting that the hover-fly *Episyrphus* also joins this group when it uses a horizontal stroke plane. The ladybird *Coccinella* and crane-flies *Tipula*, however, have values of $\overline{\Lambda}$ between 5 and 6.

4.2. *The Wagner effect*

In one of the first major breakthroughs in unsteady aerofoil theory, Wagner (1925) analysed the growth of circulation around a section when the quasi-steady circulation changes abruptly. This may be regarded as the kernel of unsteady processes because, in the limit, the effects of any arbitrary motion can be reduced to a series of infinitesimal step changes in the quasi-steady circulation. His analysis applies directly to the growth of circulation around a section suddenly set into translational motion, which was crudely modelled in the preceding section, and is known as the *Wagner effect*. Figure 5*a* shows his results for the growth of circulation and lift, expressed as fractions of the quasi-steady values, as a function of the non-dimensional distance λ. The wake vorticity has a strong influence when λ is small, as expected, and even after six chords of travel the circulation and lift are only 90% of the quasi-steady values. Walker (1931) experimentally confirmed Wagner's theory for a symmetrical profile (RAF 30) at an angle of attack well below stall, and his results are indicated by the dashed line.

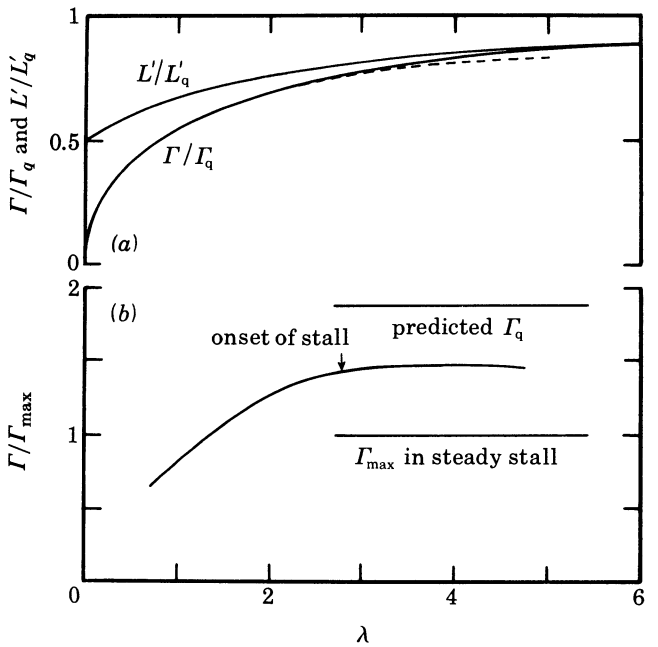

FIGURE 5. (*a*) The growth of circulation and lift, expressed as fractions of the quasi-steady values, as predicted by Wagner's theory. The dashed curve shows Walker's (1931) experimental results. (*b*) Delayed stall at an incidence greater than the steady stall angle, from Francis & Cohen (1933). Γ grows towards the predicted Γ_q instead of the maximum value Γ_{max} limited by steady stall, until the first signs of stalling are detected.

In unsteady aerofoil theory, vorticity shed into the wake always causes the instantaneous circulation to change more slowly than Γ_q. This is clearly evident for Wagner's effect, where the induced circulation from starting vorticity reduces Γ from the quasi-steady expectation at the beginning of motion. Similarly, if the angle of attack is suddenly decreased for an aerofoil, then Γ slowly decays to the new value of Γ_q. When the quasi-steady parameters change gradually with time, the wake vortices are weak and do not significantly affect the flow around the section; thus Γ is close to Γ_q and the quasi-steady approximation is valid. The instantaneous circulatory lift for unsteady motion can be derived from the time rate of change of momentum for the entire bound and wake vortex system. The lift is *not* simply equal to $\rho U\Gamma$ in unsteady

motion; figure 5*a* shows that the lift is 50% of the quasi-steady value at $\lambda = 0$, even though the instantaneous circulation is zero at that point. Like the circulation, the lift sluggishly follows the quasi-steady value because of wake vorticity.

4.3. *Gross circulation changes in hovering*

The circulation around a wing element undergoes dramatic changes during each half-stroke of hovering flight. Consider first the case of a horizontal stroke plane, as in figure 6*a*. Because the flapping velocity is reversed each half-stroke, the sense of the circulation must also reverse to provide the required vertical force. If the wingbeat is symmetrical, then the circulation on the upstroke $-\Gamma$ is equal but opposite to that on the downstroke Γ, and it must pass through

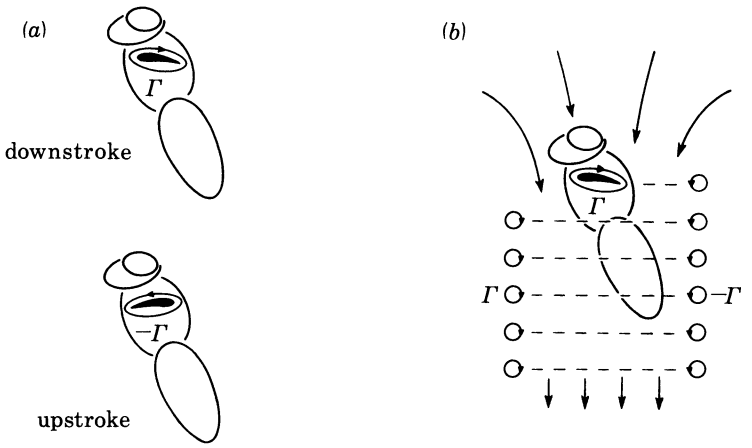

FIGURE 6. Gross circulation changes for hovering flight with a horizontal stroke plane. (*a*) The wing circulation reverses sign each half-stroke. (*b*) The shed vorticity corresponding to these changes in circulation forms the vortex wake in this two-dimensional view. The stopping and starting vortices provide a boundary around the downwash jet.

zero during the transition at either end of the cycle. At the beginning of the downstroke, starting vorticity of strength $-\Gamma$ is shed as the circulation grows around the section. The circulation must be lost at the end of the downstroke, and is shed in the form of a 'stopping vortex' of strength Γ. This process is repeated on the following upstroke, but the signs of the circulations and the placement of 'starting' and 'stopping' vortices are reversed. The vortex pair generated each half-stroke moves downwards, and forms the vortex wake that extends below the animal. Figure 6*b* shows a two-dimensional view of this wake, and the full three-dimensional structure will be considered in paper V. For animals that use an inclined stroke plane, the circulatory lift is insignificant on the upstroke, and substantial vortex pairs are only created on the downstroke.

If the quasi-steady circulation is roughly constant during a half-stroke, the instantaneous circulation should grow steadily in a manner similar to the Wagner effect. The total distance $\overline{A}$ travelled by the wings is small, so the circulation and lift should be well below the quasi-steady expectation. The effect will be especially harmful for animals that use an inclined stroke plane, where $\overline{A}$ is typically less than 3. For animals that use a horizontal stroke plane another difficulty arises, because each starting vortex is very close to the stopping vortex of the preceding half-stroke.

They are both of the same sense, and may even be shed together as one large vortex during rotation, so the downwash experienced by the wing should be nearly double the usual value and the Wagner effect will be aggravated. Finally, there are problems with the decay of circulation as well as the growth of it. Since the Wagner effect is symmetrical with regard to changes in the quasi-steady circulation, the shedding of vorticity at the end of a half-stroke should be just as slow as at the beginning. Thus the circulation will decay as gradually as it grows, and will interfere with the build up of circulation on the following half-stroke. To prevent this interference, some mechanism is required that sheds the vorticity more rapidly than the considerations so far.

4.4. *Virtual mass forces*

Additional forces on an aerofoil arise in unsteady theory because of the virtual wing mass, which was introduced in paper II. The contribution of the virtual mass forces to the section lift is usually derived assuming that α is small, and is given by

$$L' \approx \tfrac{1}{4}\rho\pi c^2\left[\frac{\mathrm{d}^2 z}{\mathrm{d}t^2} - \frac{\mathrm{d}\omega}{\mathrm{d}t}c(\hat{x}_0 - \tfrac{1}{2}) + \omega U\right], \tag{19}$$

where z is a distance measured perpendicular to the flight path, positive downwards (see Fung 1969). The virtual mass per unit span, $\frac{1}{4}\rho\pi c^2$, is the mass of air set in motion when the section accelerates perpendicular to its chord: the centre of virtual mass is located at the mid-chord $\frac{1}{2}c$. Thus the first two terms in the square brackets represent the force associated with acceleration of the centre of virtual mass normal to the flight path because of linear and rotational motion, respectively. The third term is a sort of quasi-circulatory lift, that results from an 'apparent' circulation produced as the virtual mass rotates with the section.

Osborne (1951) suggested that virtual mass forces may play an important role in flapping animal flight. Both $\mathrm{d}^2z/\mathrm{d}t^2$ and $\mathrm{d}\omega/\mathrm{d}t$ are periodic functions with a mean value of zero over a half-stroke, however: the mean acceleration of the section normal to the flight path must be zero. Thus the first two terms of equation (19) cannot contribute to the mean wing forces in flight. I cannot prove by inspection that the mean value of ωU is also zero over a half-stroke, but it must be very small because of the symmetry of the kinematics. Therefore none of the virtual mass forces will significantly alter the mean lift of the wing, although they will affect the instantaneous values. Even though the approximation of equation (19) is valid only for small α, these arguments apply equally well to a more general analysis.

Virtual mass forces also contribute to the wing drag, but the mean force is again zero because there is no net acceleration of the wing parallel to its path during a cycle. The flight muscles may not appreciate this mathematical nicety, though, if the required inertial torques at the wing base are supplied by the muscles instead of an elastic system. The 'drag' that arises from virtual mass forces is strictly analogous to the inertial force associated with accelerations of the wing mass, and can be calculated if the accelerations of the centre of virtual mass at $\frac{1}{2}c$ are known. Unfortunately, all of the data needed for this calculation could not be measured in paper III: the axis of rotation $\dot{\hat{x}}_0$ and the angle of attack α. Thus the instantaneous values cannot be estimated, but we can still calculate the work done against virtual mass 'drag', which is of primary interest. Consider first the work done in accelerating the mass of both wings at the beginning of a half-stroke. This work must equal the kinetic energy gained by the total wing mass, $\frac{1}{2}I_{\mathrm{w}}(\mathrm{d}\phi/\mathrm{d}t)^2_{\mathrm{max}}$, where I_{w} is the moment of inertia for both wings and $(\mathrm{d}\phi/\mathrm{d}t)_{\mathrm{max}}$ is the maximum angular velocity of flapping. A negative amount of work with the same magnitude

must be done to decelerate the wings at the end of a half-stroke, and this will cost metabolic energy if the muscles are used. The chord is nearly perpendicular to its motion as the wings change velocity at the ends of a half-stroke, so the virtual mass undergoes similar accelerations and decelerations. The work done imparting kinetic energy to the virtual mass is then $\frac{1}{2}I_{\mathrm{v}}(\mathrm{d}\phi/\mathrm{d}t)^2_{\mathrm{max}}$, where I_{v} is the virtual moment of inertia for both wings. (According to the definitions in paper II, I_{v} is equal to the second moment of virtual mass v_2, and I_{w} is similarly equal to m_2.)

4.5. *Applicability of unsteady theory*

In spite of the useful discussions provoked by unsteady theory, it cannot be rigorously applied to hovering animal flight. Many authors (e.g. Wagner 1925; Glauert 1929; Theodorsen 1935; Küssner 1941; Kármán & Sears 1938) have used analytical approaches to conventional unsteady problems with success, largely because of simplifying assumptions that are not tenable for our interests. The equations are linearized by considering a thin aerofoil with very small mean angle of attack and camber, moving at a constant mean velocity while subjected to infinitesimal variations of velocity and attitude. Furthermore, the wake is assumed to be planar and stationary with respect to the undisturbed air: the wake vorticity remains where it is deposited along the flight path, and does not move under its own induced velocity field. These simplifications are reasonable for normal unsteady motions such as wing flutter and, perhaps, the fast forward flight of birds. Möllenstädt (1980) provides a general review of the application of unsteady theory to bird flight, and a new three-dimensional unsteady theory for birds can be found in Phlips *et al.* (1981). The approximations of unsteady theory are hardly suitable for hovering animal flight, however. The unsteady wing motion is large in amplitude with zero mean velocity, and the wake vorticity convects downwards at a substantial speed in the jet formed by the beating wings. Modern developments in unsteady aerofoil research are attempts to relax various assumptions underlying the thin-aerofoil theory (McCroskey 1982), but the progress to date still lags far behind what is required for hovering flight. Several authors have derived unsteady theories for helicopter rotors, which are closer to our interests (see Bramwell 1976 for review), but the linearized equations and differences in wake geometry still inhibit a straightforward application of their results.

A sophisticated theory of hovering animal flight could probably be derived in a manner similar to helicopter rotors, but I think substantial progress can be made at this time using more qualitative deliberations with the mathematics firmly under control. Indeed, physical deliberations are a prerequisite to the identification of the aerodynamic features that must be incorporated in a detailed theory. We have seen that large amplitude wing rotation and the formation of leading edge separation bubbles are likely to be important aspects of hovering. The latter are particularly troublesome, and have been investigated numerically for relatively simple motions by breaking the shed vortex sheet into a number of discrete vorticies (Clements & Maull 1975; Sarpkaya 1975; Sears 1976; Kiya & Arie 1977; Katz 1981). Qualitative features of the flow pattern have been simulated quite well by this approach, but further refinements are generally needed for better quantitative accuracy. After the leading edge bubbles are satisfactorily modelled, we would have to find the vorticity distribution in the wake of the hovering animal, probably relying on numerical methods again. A complete three-dimensional iterative analysis would be required to determine the convoluted vortex structure of the wake, which will be discussed in paper V, and there is every chance that the process would not be convergent. Apart from the difficulties often encountered when representing a

PHILOSOPHICAL TRANSACTIONS OF THE ROYAL SOCIETY B BIOLOGICAL SCIENCES

wake by discrete vortex elements in numerical work, the problem is again much more complex than the analogous one for rotors.

The computing time for such a detailed unsteady theory is likely to be astronomical, and alternatives must be found. Based on some judicious physical approximations instead of mathematical ones, the vortex theory of paper V offers a means of estimating the lift production, induced power requirement and induced velocity field from the circulation around the wing elements. The induced velocity estimate is probably too crude for the calculation of the induced circulation around the wings, and hence for finding the continuous distribution of bound and wake vorticity that satisfies the unsteady motion. Although the theory does provide the basic framework necessary for an extension of the unsteady helicopter theories to hovering animal flight, such an extension would be premature with our limited knowledge about separation bubbles. Furthermore, there are other possible aerodynamic mechanisms for the generation of circulatory lift that need to be considered, and that lie outside the realm of conventional unsteady theory. The best that can be achieved at present is to identify probable aerodynamic mechanisms for hovering flight, and to postulate how the circulation around wing elements is likely to vary during the wingbeat. These postulated circulations can then be used in the vortex theory of paper V.

5. Delayed stall

Except for the discussion on stall in steady translation, the previous sections have been concerned largely with aerofoils at small angles of attack because this case is most amenable to theoretical analyses. Some very interesting experimental results have been obtained for aerofoils in unsteady motion with large values of α, though, and these are of great importance to hovering flight. Francis & Cohen (1933) repeated Walker's experiments on the growth of circulation around a section suddenly set in translational motion, but the angle of incidence was greater than the one at which the wing stalls in steady motion. The circulation grew in a manner similar to Wagner's theory for the first 3 chords of travel and then remained approximately constant up to 5 chords, when measurements ceased (Figure 5*b*). Although the experiment clearly departs from the linearizations assumed in Wagner's theory, the agreement is quite good for the first three chords of travel. At that point the first signs of stalling were detected, and the circulation began to plateau. The surprising result was that the circulation did not approach the maximum observed value for steady stalled flight, but grew for the first 3 chords towards the circulation that would be theoretically predicted by equation (2) in the absence of stall considerations.

The results of Francis & Cohen (1933) are an example of *delayed stall*: an aerofoil can travel several chord lengths at large incidences before the separation associated with stall begins, and large *transient* circulations can be developed during that period. Even though the Wagner effect was still operative, reducing the effective angle of incidence for small λ, Francis & Cohen (1933) measured circulations greater than the steady stalled value after only 1.5 chords of travel, and which exceeded that value by some 40–55 % when stall finally began. The enhanced circulation must eventually be lost as the flow separates from the upper surface and the steady case is realized, but this does not occur for at least 5 chords of travel. Maresca *et al.* (1979) have also demonstrated a delayed stall for an aerofoil at large angles of incidence executing oscillations parallel to the airstream of a wind tunnel: large circulatory lifts were measured as the aerofoil moved forward in the cycle. These corresponded to unstalled flow over the upper surface.

PHILOSOPHICAL TRANSACTIONS OF THE ROYAL SOCIETY B BIOLOGICAL SCIENCES

Rotation provides a second method of delaying stall for a translating wing. If an aerofoil in steady translation is given a slight rotational velocity with ω *positive*, then the stall is delayed until higher angles of incidence. Enhanced values of $C_{L,\max}$ are thus obtained, and they tend to increase with the rotational velocity (Kramer 1932). This phenomenon, known as *Kramer's effect*, was further investigated by Farren (1935). He also found that the aerofoil stalls at smaller incidences and that $C_{L,\max}$ is reduced for *negative* rotational velocities, that is the aerofoil rotates from angles of incidence above stall to below. It is this influence of rotation on stalling behaviour that prompted my remark in §3 that values of $C_{L,\max}$ measured under steady translation cannot be applied to the conditions of rotation and translation.

Fung (1969) summarizes the experimental results on Kramer's effect, and states that the increase in the maximum lift coefficient above the steady stall value is equal to 21.7 $\omega c/U$ for values of $\omega c/U$ greater than 0.003 (0.17° per chord of travel). The highest value tested is only 0.042 (2.4°/chord), far below the values near unity observed for hovering flight (paper III), but this still increased $C_{L,\max}$ by an impressive 0.9. Using equation (12) of the quasi-steady assumption, it can be shown that these small rotational velocities do not significantly alter C_L simply by increasing the angle of incidence at the $\frac{3}{4}$ chord point; the enhanced lift coefficients at high angles of incidence must be the result of a delayed stall instead.

The effects of large rotational velocities on model flapping wings was investigated by Bennett (1970). Although $\omega c/U$ cannot be calculated from his published data, it was probably much greater than in the experiments above. The model wing was rotated rapidly in the middle of the downstroke, which does not occur in hovering, and generated an increased lift when ω was positive. He suggested that the results were probably due to delayed stall rather than the quasi-steady rotational lift, but this cannot be determined for certain. In either case, the results are remarkable: lift was still produced at angles of incidence up to about 70°. Flow visualization studies by Rüppell (1977) on model profiles of the fulmar wing (*Fulmarus glacialis*) also indicate that stall can be delayed to very large angles of incidence when flapping wings are rotated at high velocities.

Delayed stall is the only conventional unsteady mechanism that can produce circulatory lift in excess of the maximum observed for steady motion. To some extent it removes the limitations imposed by stall on aerodynamic theories, so that predicted lifts can be attained for a brief time at large incidences. It is therefore a strong candidate for producing the high lift coefficients required of animals hovering with an inclined stroke plane (papers I and VI), where C_L is too large to be explained by quasi-steady high lift devices, such as the alula, separated primaries and strong cambering. Delayed stall permits operation of the wings at large incidences over the short distance travelled in each half-stroke, generating enhanced circulations to compensate for the Wagner effect. As the angle of incidence increases towards the end of a half-stroke, Kramer's effect may also be involved in the delay of stall. The only question is whether delayed stall can be effective for wings that already show a gradual stall in steady motion: Vogel (1967) suggested that Kramer's effect would be ineffective for *Drosophila* wings because they do not stall in the usual manner found at high *Re*, and still produce lift at large incidences even in steady motion. However, more recent numerical studies on the flow around thin aerofoils at high incidences reveal that steady 'stall' can be a very dynamic process (Sarpkaya 1975; Kiya & Arie 1977; Katz 1981). Leading edge bubbles periodically grow and then break away from the upper surface, alternating with the periodic shedding of vorticity of the opposite sense from the trailing edge; a highly organized vortex wake structure develops, similar to a Kármán vortex

PHILOSOPHICAL TRANSACTIONS OF THE ROYAL SOCIETY B BIOLOGICAL SCIENCES

street. The force coefficients vary periodically with the vortex shedding, and peak values can be considerably in excess of the means. Over the short distances travelled by the wings during hovering, it should be possible to achieve larger leading edge bubbles, and hence greater circulatory lift, than those suggested by the mean results from steady stall. I therefore think that delayed stall will be quite effective for the insect wings, contrary to Vogel's conclusion, but experimental verification is obviously required.

6. Pronation and supination

6.1. *The fling mechanism*

Until now the discussion has primarily centred on the aerodynamic events associated with translation of the wing during a half-stroke. If strong vortex patterns are produced during the rapid rotations of pronation and supination, then this picture may need modification on the following half-stroke. Weis-Fogh (1973) proposed such a scheme with a new circulatory lift mechanism, the *fling*, to explain the high lift coefficients required for flight of the small wasp *Encarsia*. Before beginning a downstroke the wings are 'clapped' dorsally with longitudinal wing axes horizontal, as seen in vertical section in figure 7*a*. The wings then 'fling' open about their trailing edges, and the flow of air into the opening gap creates equal but opposite circulations around the wings. The magnitude of this circulation in an inviscid fluid has been analysed by Lighthill (1973), who found that the circulation varies with the half-angle β between the wings:

$$\Gamma = \omega c^2 g(\beta), \tag{20}$$

and the function $g(\beta)$ is presented in figure 7*b*. The wings separate when β is about $\frac{1}{3}\pi$ at the end of the fling motion, and this results in a circulation of $0.69\,\omega c^2$. Lighthill suggested that viscous effects would modify his model a little, and form a leading edge bubble that slightly enhanced the circulation predicted by inviscid theory.

The fling mechanism commands a great conceptual interest because it creates a circulation around each wing before, and independently of, translation. As the wings separate and begin the downstroke a circulation already exists around each wing, created by the *rotational* motion, and the bound vortex of one wing may be considered as the starting vortex of the other. In doing this, the fling eliminates the gradual growth of circulation in the Wagner effect and enables circulations to be generated that are greater than the maximum value found in translation. Ellington (1975) applied Lighthill's analysis to the flight of *Encarsia*, and demonstrated that the fling circulation was larger than that given by $C_{\mathrm{L,\,max}}$ and would produce sufficient circulatory lift for flight. The fling mechanism is not merely of parochial interest, however: Furber & Ffowcs Williams (1979) have investigated its application to the design of turbomachinery.

The fling mechanism has been experimentally tested by Bennett (1977) and Maxworthy (1979), and both have verified the creation of large circulations during the fling motion. Maxworthy's measurements show that the circulation at the end of the fling is some three times that predicted by Lighthill. This circulation is primarily due to vorticity concentrated in an enormous leading edge separation bubble (figure 8, plate 1), much larger than Lighthill envisaged, and which contains all of the vorticity shed from the leading edge during the fling motion. It may be considered as 'attached' to the wing because it follows the wing motion,

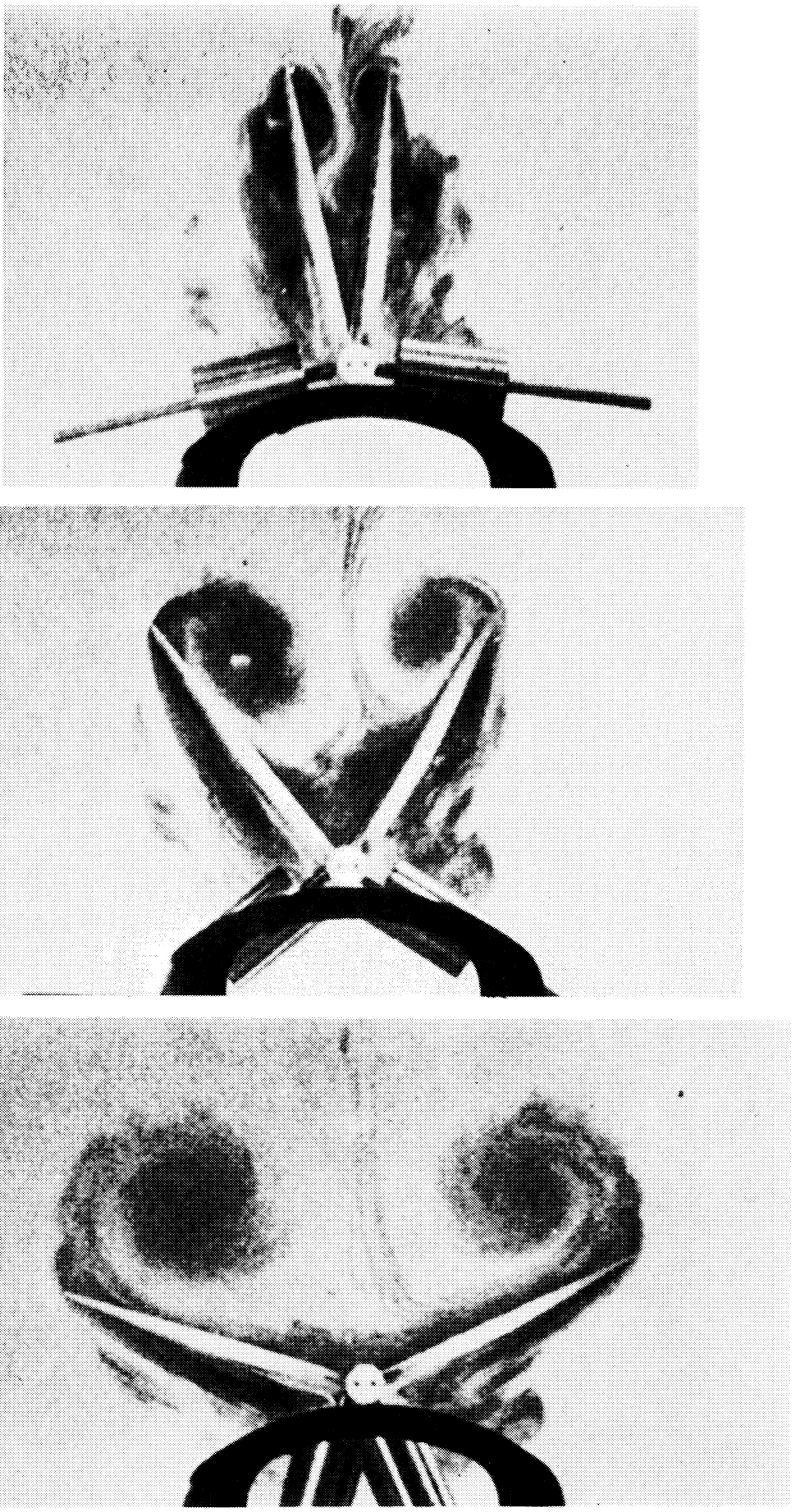

FIGURE 8. Operation of the fling in a viscous fluid. Vorticity shed from the leading edges rolls up into large leading edge separation bubbles, which contain most of the circulation created by the fling mechanism. From Maxworthy (1979).

(*Facing p.* 101)

PHILOSOPHICAL TRANSACTIONS OF THE ROYAL SOCIETY B BIOLOGICAL SCIENCES

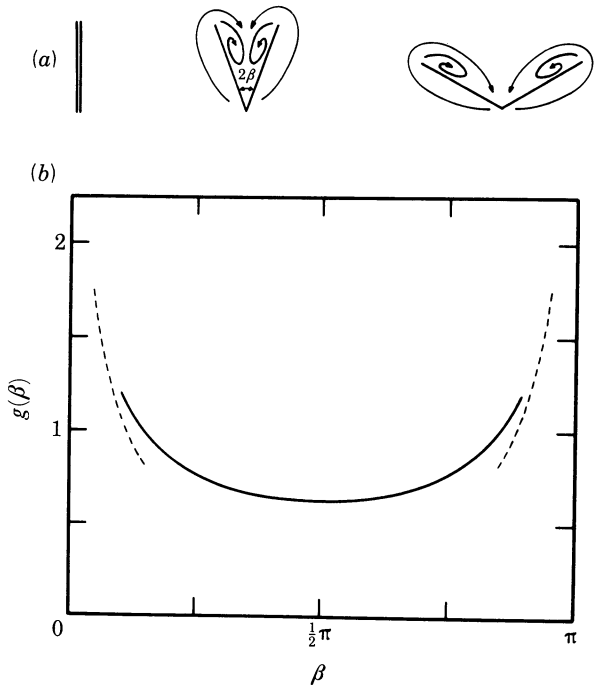

FIGURE 7. (*a*) The air motion and circulation created by the fling mechanism. β is the half-angle between the wings. (*b*) The function $g(\beta)$ from Lighthill (1973). The dashed lines represent a small angle approximation.

so the circulation must be defined around a curve enclosing both the wing and the bubble. In this manner, the bubble vorticity increases the net circulation created around each wing by the fling.

The prominent leading edge bubble must be regarded as an integral part of the fling mechanism in a viscous fluid. Its formation is assured because of the sharp local deceleration as the flow rounds the leading edge, and it must grow in strength as vorticity shed from the leading edge accumulates during the fling. While the bubble and its induced velocity field strengthen, the mean velocity of air flowing into the gap decreases – the mean inflow velocity is inversely proportional to β. Thus the bubble progressively dominates the flow over the upper wing surface, disrupting the streamline pattern assumed in the inviscid analysis. Edwards & Cheng (1982) have extended Lighthill's analysis to include leading edge vortex shedding, and their results compare reasonably well with Maxworthy's experiments. The circulation around each wing is primarily due to the concentration of shed vorticity in the bubble, and hence it tends to *increase* with the opening angle instead of decrease, as Lighthill's analysis predicted.

What happens to the enhanced circulation during the subsequent downstroke? Because it is greater than the circulation that can be maintained in steady translation, some vorticity must eventually be shed from the wing. The leading edge bubble may remain attached to the upper surface during the brief downstroke, however, through the action of delayed stall in translation and Kramer's effect in rotation at the end of the downstroke. The bubble may grow in length during this time, finally shedding vorticity when it reaches the trailing edge. If this does not happen before the end of the downstroke, then most of the fling circulation contained in the bubble should persist for the half-stroke and generate sufficient lift for flight. Bennett (1977) found that the circulatory lift abruptly decreases after about 1 chord of travel, though,

indicating a severe stall with complete flow separation from the leading edge. I have commented on Bennett's experimental evaluation elsewhere (Ellington 1980), and presented objections to his modelling. Maxworthy (1979) investigated the persistence of the fling circulation more carefully at Reynolds numbers more appropriate to the mechanism (13000 and 32 instead of Bennett's 83000). By using a three-dimensional flapping model, he determined that the fling circulation does persist during the entire downstroke, and that the three-dimensional vortex shedding pattern helps to stabilize the bubble.

6.2. *The peel*

Paper III described a kinematic variation of the fling found in the Lepidoptera and *Drosophila*, called the *peel*: the wings curve along the chords and the separation point moves smoothly from leading to trailing edges, rather like pulling two pieces of paper apart by their leading edges. This is crudely illustrated in figure 9*a*, but the resolution limits of the cine films

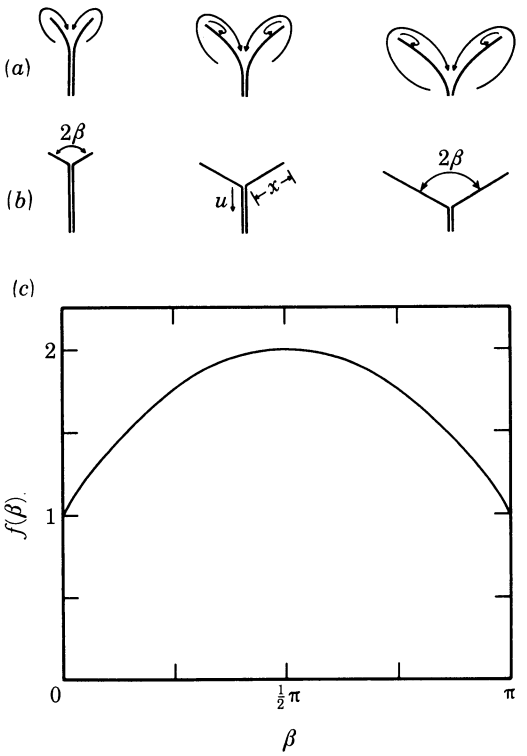

FIGURE 9. (*a*) The air flow and circulation created by the peel mechanism. (*b*) The flat peel model and (*c*) the circulation function $f(\beta)$.

prevent a more accurate representation. In the absence of a better description, Charles Williamson and I have analysed the inviscid flow that would be produced by a 'flat peel', which is shown in figure 9*b*. Although only a rough approximation to the real motion, this model incorporates most of the salient features of the peel. The chords unzip with a velocity u that may vary with time, and the exposed chord length x remains flat with a constant half-angle β. The circulation Γ around the exposed chord is

$$\Gamma = uxf(\beta), \tag{21}$$

where $f(\beta)$ is given in figure 9*c*.

The flat peel is remarkably different from Lighthill's fling model. The circulation around the exposed chord increases linearly with x and will therefore grow during the flat peel, instead of decay as in his fling. This growth is to be expected because the flow field is geometrically similar at all times. A leading edge bubble will undoubtedly form, but it should not assume such a dominant influence: the mean inflow velocity is independent of x, so the shed vorticity will be swept steadily along the lengthening upper surface, distributing the vorticity evenly instead of allowing it to roll up into a large bubble. Thus the flow pattern in a viscous fluid should not deviate too much from the inviscid model for this case. Finally, the flat peel works best when β is close to a right angle, whereas the fling creates the most circulation when β is small. The circulation around each wing at the end of a flat peel would be 1.89 uc, using β equal to $\frac{1}{3}\pi$ as before. To compare the flat peel with the fling we will assume that u and ω are constant and that the motions last the same amount of time, giving $u = \omega c/\beta$. The circulation created by the flat peel is then 2.6 times that predicted by Lighthill's model, and nearly equal to the values measured experimentally by Maxworthy and predicted by the model of Edwards & Cheng.

The flat peel, in short, overcomes many of the problems associated with the fling. It creates large circulations without the formation of an enormous leading edge bubble, which may have but marginal stability in the subsequent half-stroke, and the simple inviscid analysis should correspond more closely to the real case. Williamson has recently improved the model by combining it with the fling in a composite model, letting the exposed chord lengths rotate after they peel apart. This is a more accurate model of the peel motion and yields even greater circulations. Details will be published elsewhere, along with the theory of the flat peel (Williamson & Ellington 1984).

6.3. *The clap*

Before a pair of wings can begin a fling or peel, they must touch along their upper surfaces. This is accomplished by a *clap* motion at the end of the upstroke, described by Weis-Fogh (1973) for *Encarsia* and shown in figure 10*a*. As the wings decelerate at the end of an upstroke, α increases, the leading edges touch, and the wings clap together in a reversal of the fling motion. My films of the Lepidoptera reveal that their clap is more akin to a reversal of the peel, however. The meeting point between the wings moves steadily towards the trailing edge, as in figure 10*b*. The relatively rigid wings of small insects, including *Encarsia*, probably compromise with a double-clap, which is a reversal of the double-fling described in paper III.

The aerodynamic implications of the clap are very interesting, and were first considered in Ellington (1980). If we neglect any circulation remaining around the wings from the upstroke for the moment, then the clap would create the jet motion indicated by the dashed lines in figure 10*a*. The vorticity shed from the trailing edge should roll up into a large bubble, which is probably true for the reversed peel as well: the flow outside the gap moves slowly and is easily dominated by the shed vorticity. Thus in a two-dimensional view, the clap produces a vortex pair corresponding to a brief downward jet of air, and the wings must experience an upward reaction force to this jet. Maxworthy (1981) has published a flow visualization photograph of a pair of model wings executing a clap, confirming the features of this flow. The mean vertical force from the clap can be estimated roughly using a reversed flat peel model, which avoids the difficulties with infinite outflow velocities when β approaches zero in Weis-Fogh's model. The mass of air per unit span $\rho\beta c^2$ between the wings gains a velocity u in the duration c/u of the

clap, and the mean force per unit span $\bar{F}'$ corresponding to this change in momentum is $\rho\beta cu^2$. This slightly overestimates the vertical force of the clap because some momentum is wasted in the spreading of the jet, but the difference will be small. The force per unit span should be integrated along the wing length to obtain the total mean force $\bar{F}$ of the clap, but we can simply multiply it by R and use the value of the mean chord $\bar{c}$ for a first approximation. This gives

$$\bar{F} = \rho\beta\bar{c}u^2R = \rho\omega^2\bar{c}^3R/\beta, \tag{22}$$

where the expression $u = \omega c/\beta$ relating the fling and the flat peel is used for the right-hand side. Substituting data from Weis-Fogh (1973) into this equation shows that the mean jet force of the clap in *Encarsia* is roughly equal to the mean lift force required of the wings for weight support.

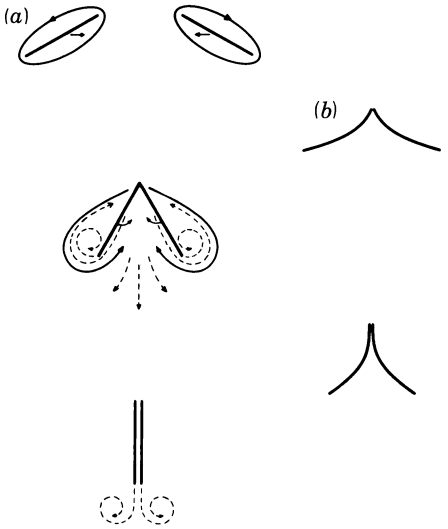

FIGURE 10. (*a*) Possible flow patterns during the clap. The solid curve indicates the circulation already around each wing as the clap is approached. The air motion that would be produced by the clap if this circulation did not exist is given by the dashed lines. (*b*) The clap is more similar to a reversed peel than a reversed fling for the Lepidoptera.

Now consider the influence of the circulation already existing around each wing at the end of the preceding upstroke, shown by the solid curves in figure 10*a*. This circulatory motion is in the opposite direction to that which would be produced by the clap, and the two will cancel each other to some extent. If the existing vorticity does negate that produced by the clap motion, then the net vorticity shed from the trailing edge may be zero during the clap: each wing annihilates the other's stopping vortex. The jet that would be produced by the clap can then be interpreted as a continuation of the downwash produced by the wing lift during the upstroke. In this manner, the wings generate circulatory lift until they are completely clapped together, at which time the circulation disappears. Whether one wishes to view the clap as a mechanism for producing a momentum jet or as a method of extending the upstroke circulatory lift does not matter for *Encarsia*, since the mean force is the same in either case: they are simply two ways of interpreting the same phenomenon. It would certainly be possible to obtain an enhanced vertical force from the jet of a robust clap, and vorticity would then be shed from the trailing edges to form the jet boundary. A more conservative prediction, which appears to be true for *Encarsia*, would balance the clap and upstroke vorticity so that the wing lift is unchanged.

6.4. *Isolated rotation and the flex mechanism*

The rotational mechanisms discussed so far offer a unique alternative to the picture of wake vorticity in hovering flight presented in figure 6*b*. The ideal use of these mechanisms, suggested by Lighthill (1973), consists of a clap and fling (or peel) at either end of the cycle. No vorticity would be shed from the trailing edges, and the starting and stopping vortices would be absent: the vortex wake would contain only the circular trailing vortices produced by the three-dimensional motion (paper V). Thus the problems of gradual growth and decay of circulation are circumvented, and the wings generate full circulatory lift throughout the cycle. These problems still exist, however, for a wing in *isolated* rotation at the ends of the wingbeat – pronation and supination without any interference from the image wing. The pattern of shed vorticity must then agree with figure 6*b*, but details of the shedding process are unclear and have not been investigated yet. These details may be of prime importance, though, and warrant the following speculation.

I suggested in §3 that the increase in the rotational component of circulation Γ_r towards the end of a half-stroke may offset the decrease in the translational component Γ_t, resulting in a nearly constant value of the quasi-steady circulation Γ_q. If this is the case, then no vorticity will be shed as the wing decelerates and begins rotation. To test this proposition, consider the *mean* rotational circulation $\bar{\Gamma}_r$ demanded during pronation or supination and the *mean* translational circulation $\bar{\Gamma}_t$ needed for a half-stroke. $\bar{\Gamma}_r$ is approximately given by $\frac{1}{2}\pi c^2\bar{\omega}$, using equation (10) and by assuming that $\hat{x}_0$ equals $\frac{1}{4}$. Most of the translational circulation occurs in the middle of each half-stroke, when α' is nearly constant, so $\bar{\Gamma}_t$ can be estimated from equation (2) as $\pi c\bar{U}\sin\alpha'$, using the value of α' in the middle of the half-stroke. The mean flapping velocity $\bar{U}$ of a wing element is given by $\hat{r}\bar{U}_t$, where $\hat{r}$ is the non-dimensional radial position and $\bar{U}_t$ is the mean wing tip velocity. By using the mean value of the chord $\bar{c}$ as well, we can therefore write

$$\bar{\Gamma}_r/\bar{\Gamma}_t \approx \bar{\omega}\bar{c}/\bar{U}_t 2\hat{r}\sin\alpha'. \tag{23}$$

When data from paper III is inserted into the equation this ratio is about 0.6 to 1.3 at the wing tip ($\hat{r} = 1$) and thus around 2 at the middle of the wing. Many approximations have gone into this estimate, but the general conclusion should not be in error: the mean circulation associated with rotation at the ends of the cycle is comparable with, if not greater than, the circulation corresponding to translation of the wing. From these mean values we may infer that the magnitude of Γ_r is sufficient to prevent the loss of any existing circulation at the end of a half-stroke and, in fact, probably increases it.

Although enhancing the circulatory lift at the end of a half-stroke, this complicates events considerably at the beginning of the following one, when the existing vorticity *and* new starting vorticity (of the same sense) must be shed before the required circulation can grow around the wing. If rotation is completed without loss of existing circulation, then the growth of new circulation in the next half-stroke will be seriously delayed by an exaggerated Wagner effect while the necessary shedding occurs. There might be a way around this, however, if the rotational circulation is indeed greater than Γ_t. If it is assumed that this is true, the existing circulation will remain unchanged until ω exceeds a certain value. Γ will begin to increase at that time, and vorticity of the opposite sense must be shed to satisfy Kelvin's circulation theorem: this vorticity is, in fact, the 'starting vortex' for the additional circulation from rotation. Shedding will probably begin near the middle of rotation, when the wing is

perpendicular to the stroke plane. The vorticity would normally be shed from the trailing edge because of its greater velocity and shear stresses, arising from wing rotation about an anterior axis. The wing *flexes* at this time, however; the trailing edge is almost stationary while the leading edge continues rotation. As shown in figure 11, this may promote shedding at the leading instead of the trailing edge. The increase in circulation $\Delta\Gamma$ is thus balanced by shed vorticity of strength $-\Delta\Gamma$ in a separation vortex at the leading edge. Meanwhile, the 'bound' vorticity is likely to roll up and accumulate as it flows around the stationary trailing edge. The wing then begins to accelerate into translation as it unflexes, and the leading edge bubble should attach to the upper surface while the other vorticity is left behind as a combined stopping and starting vortex.

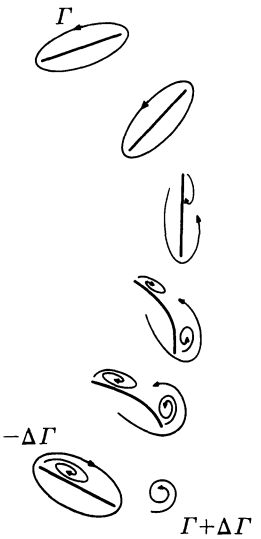

FIGURE 11. The vorticity patterns suggested for the flex mechanism in isolated rotation. See text for explanation.

This mechanism is highly fanciful and speculative, but it is the most favourable aerodynamic interpretation I can concoct for the complicated events during isolated pronation and supination. Vorticity of the correct sense for the *following* half-stroke accumulates in a separation vortex near the leading edge, just as in Maxworthy's fling experiments, and this vortex should attach to the wing at the beginning of translation. If most of the opposite vorticity has also rolled up into a vortex at the trailing edge, it will have already been 'shed' as the half-stroke commences. The wing will then have a net circulation of the required sense, provided by the leading edge bubble, and immediately experience circulatory lift. The Wagner effect should be greatly reduced, perhaps even eliminated, if the net circulation is sufficient for the new half-stroke.

I suppose that a catchy name must be coined to follow tradition, and therefore dub this the *flex mechanism* in honour of the role of wing flexing in assuring that shedding takes place at the proper edges. The flex mechanism relies on the *gross* vorticity changes produced by rotation, and uses the wing flexing to *control* the pattern of vortex shedding. It is thus quite different from the 'flip' mechanism of Weis-Fogh (1973), which was introduced in paper III. By neglecting the gross effects of rotation, he suggested that the flexing motion itself would produce important vorticity during pronation in the manner of a clap, or reversed fling, along the flexion line of the wing. The wing unflexes before the end of pronation, however, so the clap is immediately

followed by a fling along the flexion line. The vorticity created around the wing halves by these two motions must cancel out, and the net effect is zero. Because of this simple objection, I cannot believe that the 'flip' is a plausible mechanism.

Nachtigall (1979*b*) has also suggested that *gross* rotation of the wing could produce circulation for the following half-stroke, but details of the pattern of vortex shedding are not made clear. He proposes several other unsteady flight mechanisms as well, based on a detailed kinematic analysis of the fly *Phormia* in fast forward flight. In general, these mechanisms rely on brief kinematic variations and are unlikely to enhance the mean lift substantially over a wingbeat cycle. Buckholtz (1981) measured the instantaneous forces on a blowfly tethered in a wind tunnel, and noted a surprising lack of higher harmonics in the forces. This indirectly suggests that Nachtigall's other unsteady mechanisms could play no more than a minor role during flight.

Wing flexing is not absolutely essential for the creation of useful vorticity during isolated rotation; the general formulation of the mechanism only requires that the trailing edge be stationary when the circulation begins to increase because of rotation. (This may be accomplished, for instance, with a rigid wing rotating about the trailing edge.) Special problems arise for animals hovering with an inclined stroke plane because the upstroke circulation is small, if not zero, and hence will increase almost as soon as pronation begins. For these animals the trailing edge must become stationary near the start of pronation if shedding is to occur at the leading edge, creating a separation bubble that can be used on the subsequent downstroke. The kinematic results for the hover-flies in figures 9, 10 and 11 of paper III are particularly interesting in light of this. When hovering with a horizontal stroke plane (figure 9, part III), the middle of pronation lies just between the half-strokes; however, pronation is *delayed* and overlaps the beginning of the downstroke when the stroke plane is inclined (figures 10 and 11, part III). Given the same wing flexing, this delay of pronation causes the trailing edge to become stationary at an earlier point in rotation because of the additional motion from translation. This phase shift effectively partitions the rotational vorticity between upstroke and downstroke: when pronation is delayed more vorticity is shed at the leading edge, creating the larger downstroke circulation required for hovering with an inclined stroke plane. A phase *advance* of supination is also indicated on the hover-fly figures, which would use the rotational vorticity to maintain the large downstroke circulation instead of creating new circulation for the upstroke. At the end of supination all of the downstroke circulation must be shed as a stopping vortex, forming a vortex pair with the starting vortex from the beginning of the downstroke. The direction in which the pair is finally shed might be controlled by the final angle at the end of supination, providing an exquisite control over the resultant aerodynamic force vector. This may explain the extreme manoeuvrability of the 'true' hover-flies and dragonflies hovering with an inclined stroke plane.

Savage *et al.* (1979) have studied the flow patterns and inviscid forces produced by a two-dimensional flat plate model simulating the wing motion of a dragonfly hovering with an inclined stroke plane. Based on the low-speed film data of R. Å. Norberg (1975), they used an 'idealized' wing motion obtained by dividing the kinematics into separate phases: (i) pronation about the leading edge or mid-chord; (ii) an initial rapid translation in the downstroke (the 'scull'); followed by (iii) a much slower translational phase (the 'pause'); (iv) supination about the leading edge; and (v) an upstroke with uniform velocity. The 'scull' and 'pause' phases of the downstroke are unlike any wing motion previously described for an insect, though, and

cannot be seen in the high-speed film results of Chadwick (1940) for a tethered dragonfly *Ladona exusta*; high-speed films of free hovering flight are obviously required to resolve the downstroke motion. Savage *et al.* (1979) found that individual vortex pairs, corresponding to 'starting' and 'stopping' vortices, were created by each phase of the cycle. This is to be expected because the kinematic phases were separated, and results in a very complicated vortex wake instead of the ideal one suggested above for properly coupled rotations and translations. They did observe robust vortex shedding during rotations, however, that was comparable in strength to the shedding during translation. They also found that a strong leading edge vortex formed during the rapid 'scull' on the downstroke, and it was not shed during the following 'pause' period; this may be interpreted as a 'delayed stall' in translation according to the discussions of §5.

6.5. *The rotation series*

An isolated rotation is normally observed for pronation with an inclined stroke plane, and for supination in general. The pronating wings are usually separated by less than a chord length when the stroke plane is horizontal, though, and this may also occur in supination for some

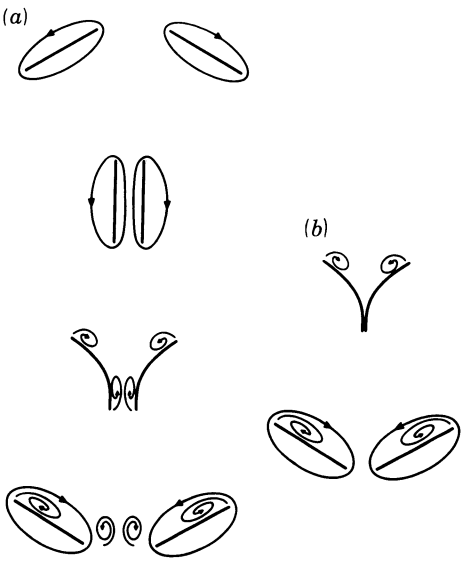

FIGURE 12. (*a*) The near clap and fling (or peel). Because of the small separation between the wings, the vortex shedding of the flex mechanism is accentuated. (*b*) The partial fling (or peel) should create even larger circulations.

insects. This motion was described in paper III as a *near* clap and fling (or peel) and is shown in figure 12*a* in this paper; the wing motions are symmetrical about a vertical plane, and the flow patterns are mirror images as well. The flow velocities between the wing and the image plane are increased because of the interference, which will promote the shedding of vorticity from leading and trailing edges. This will be especially useful in forming shed vortices at the trailing edges as the flow is sucked through the small gap, so the near clap and fling may enhance the shedding pattern proposed for isolated rotation and should result in greater net circulations as translation begins.

As the separation distance decreases between the rotating wings, they begin to touch along the posterior region of the chords in the latter half of rotation, producing a *partial* fling or peel (figure 12*b*). The clap phase, however, is not very different from the near clap. The circulation

created around each wing during the brief fling or peel may increase the strength of the vortex bubble at the leading edge and/or annihilate some of the opposite vorticity from rotation. The details of this are difficult to envisage, but the net result might be an increased circulation as the next half-stroke begins, with little or no vorticity shed from the trailing edge.

We now have a complete series of rotational mechanisms if these speculations are even close to the truth, but much experimental work is obviously required before this is known. The vorticity produced in rotation must play an important role in hovering insect flight and, in the light of the generally dismal performance of conventional unsteady effects, I think an optimistic interpretation can be pardoned at this time. The key assumption throughout is that the strength of vorticity associated with rotation is greater than that in translation, which is supported by the crude comparison of mean values. This allows full circulatory lift to be realized at the end of a half-stroke because the quasi-steady circulation remains nearly constant until about the middle of rotation. If a complete fling or peel then occurs, circulation is created around each wing in a straightforward manner for use on the following half-stroke. Otherwise, the rotational motion must be carefully manipulated to position the existing and newly created vorticity correctly. The leading edge vortex will almost certainly attach to the wing in translation, so the net circulation at the beginning of the half-stroke will be the difference between that vorticity and any opposite vorticity not already shed at the trailing edge. When the wings are close together this trailing edge shedding may be accentuated, giving greater net circulations. If the circulation is sufficient for flight, then it will not increase during the following half-stroke and the Wagner effect might be eliminated. Furthermore, the circulatory lift can be controlled by relatively small changes in the separation distance between the wings, as suggested in paper III.

7. Final comments

7.1. *Lift*

The deductions in this paper are too tentative even to consider them as 'conclusions'. Physical intuition is often an unreliable tool in aerodynamics, and we must await anxiously the results of experimental investigations. It seems certain, though, that the lift forces used in hovering flight are of a circulatory, instead of virtual mass, origin. Much of the circulation may be attributable to the vorticity in leading edge separation bubbles, which must form around the thin insect wings at low Reynolds numbers. Separation bubbles are just as likely to occur in rotation as translation, providing vorticity that may be useful in the following half-stroke. The flow field around the wings will be governed largely by the bubbles, so the exact profile shape is probably not very important.

Animals that hover with an inclined stroke plane are especially worthy of attention because, as discussed in paper I, the mean lift coefficient $\bar{C}_{\mathrm{L}}$ required on the downstroke is greater than the maximum possible in steady motion $C_{\mathrm{L,\,max}}$. This implies that delayed stall *must* be operative to *maintain* the enhanced circulation corresponding to the extra lift. The large downstroke circulation could even be *created* by the delayed stall of translation, when the results of Francis & Cohen (1933) and Savage *et al.* (1979) are considered. If such is the case, then the circulation grows during translation in a manner similar to that found by Francis & Cohen (1933), reaching a peak value greater than that associated with $C_{\mathrm{L,\,max}}$. This is particularly likely for birds and bats because rotational effects may be small for them: the extent of rotation is reduced by anatomical constraints, and the rotational velocities should be correspondingly less.

PHILOSOPHICAL TRANSACTIONS OF THE ROYAL SOCIETY B BIOLOGICAL SCIENCES

The largest values of $\omega c/U$ in paper III are found for the hover-flies using an inclined stroke plane. This indicates a more important role for rotational effects. For them, and perhaps the dragonflies, the circulation demanded on the downstroke may be created by the vorticity of rotation at these relatively high angular velocities. Indeed, there are few differences between the hover-fly kinematics for a horizontal and inclined stroke plane that can explain the enhancement of downstroke circulation: $\omega c/U$ increases in the latter case because of the reduced stroke angle Φ, the downstroke angle of attack α is 10–15° larger, and pronation and supination overlap the downstroke translation. The increase in α will be partially offset by the greater induced velocity associated with an inclined stroke plane (papers V and VI). This will result in a small change in the effective angle of attack α_r that is probably insufficient to produce the extra lift. Furthermore, the decrease in Φ reduces the flapping velocity and circulatory lift, worsening the Wagner effect, so it is unlikely that the enhanced circulation can be generated by a delayed stall in translation. The relatively high angular velocity of pronation and its phase shift are thus the most probable means of creating the large downstroke circulation. This would generate circulation *before* translation, possibly eliminating its gradual growth in the usual Wagner effect, and delayed stall would prevent the loss of this circulation whenever the translational velocity is small.

We may expect the aerodynamics for a horizontal stroke plane to be similar because the kinematics differ but little. Circulation can certainly be established before translation by a fling or peel, and this is also likely for a partial or near fling (or peel). The effectiveness of the flex mechanism, however, is unknown at present. If it is viable, then all of the insects in paper III can create upstroke and downstroke circulation during the rotational periods. Otherwise, the circulations will have to grow conventionally in translation. The rotational phases may still perform a vital function in rapidly shedding the existing circulation, though, so that the build up of new circulation on the following half-stroke is not fouled. Maxworthy's (1979) three-dimensional flow visualization hints at a rapid shedding after supination for his model, but details of the process are lacking.

These considerations stray far from the usual quasi-steady interpretation of hovering flight. The instantaneous circulation must lag substantially behind the quasi-steady value over the few chords of translation because of the Wagner effect, unless the circulation is pre-established by rotation. In either case, it will not follow the quasi-steady prediction. Delayed stall, another unsteady effect, is probably important as well. The circulation required for rotation towards the end of each half-stroke will increase C_L as the flapping velocity decreases, provided that the wing does not stall. The results of Bennett (1970) and others indicate that stall will be delayed by rotation (Kramer's effect), permitting values of C_L in excess of $C_{L,\max}$ to be realized. This clearly violates the quasi-steady assumption, and should hold true for all the hovering insects in paper III. The assumption is further broken if the delayed stall of translation is used to create excessive circulatory lift to compensate for the Wagner effect.

The potential benefits of delayed stall and rotation should be marginal in fast forward flight, where translational velocities of the wing are enhanced by the flight speed and wing rotations are reduced; the wing travels too great a distance for delayed stall to work, and $\omega c/U$ becomes much less than unity. The storm petrel *Oceanites oceanicus* may, however, be an important exception to this general trend. The petrel 'hovers' over the water surface when feeding; it is presumed to be flying into an ambient wind (Withers 1979). The kinematics are very unusual for a bird: there is virtually no translation of the wings, only rapid pronations and

PHILOSOPHICAL TRANSACTIONS OF THE ROYAL SOCIETY B BIOLOGICAL SCIENCES

supinations. In combination with the weak wind, this motion must provide the lift and thrust satisfying the net force balance. Details of the rotational motion cannot be resolved from Withers' films, but the creation of circulation by isolated rotation must be a strong candidate for the flight mechanism involved. This is also likely for the quivering wing motion of kestrels as they 'hover' above the ground while flying into the wind.

Except for such cases, we should expect the usual quasi-steady assumption to be a reasonable approximation to the aerodynamic events of fast forward flight: angles of incidence are small and below stall, rotational velocities are relatively low, and the distance travelled during the downstroke is at least an order of magnitude greater than the chord length. The results of Cloupeau *et al.* (1979) are particularly disturbing in light of this expectation. They measured the instantaneous vertical forces produced by the locust *Schistocerca gregaria* flying in a wind tunnel, and compared their results to the quasi-steady predictions of Jensen (1956). The measured lift curves were of a similar shape to Jensen's, but approximately double in amplitude: the downstroke vertical force was larger and the upstroke smaller. They suggest that the differences are because of unsteady effects but cannot offer a more detailed explanation. In fast forward flight the locust wings behave according to all the qualifications of the quasi-steady assumption listed above. Indeed, the wing travels over 20 chord lengths during the downstroke so even the conventional unsteady effects of wake vorticity should be negligible. These baffling results might be explained by the dynamic characteristics of leading edge separation bubbles, but further experimental investigation is obviously required.

7.2. *Drag*

Little has been said about the unsteady drag forces in hovering simply because nothing is known and it is a more difficult topic of speculation than circulatory lift. The theory of paper V can be used to calculate the work done against induced drag, and a treatment of virtual mass drag forces has already been outlined, so the problem can at least be reduced to one of profile drag. The skin friction component of profile drag is often increased in unsteady motion because the boundary layer is thinner and shear stresses correspondingly greater. The pressure drag component, however, may be lower if flow separation is reduced. The two effects may cancel, giving a profile drag very close to the quasi-steady value when complete separation and stalling are absent (Maresca *et al.* 1979).

As we lack more information, we may as well apply the profile drag coefficients $C_{\mathrm{D,\,pro}}$ measured in steady motion to the analysis of hovering. Because the angle of incidence is nearly constant during the translation phases of the cycle, it is also reasonable to assume that $C_{\mathrm{D,\,pro}}$ varies but little. Thus the profile drag can be estimated by the usual quasi-steady method, if a mean value of the drag coefficient based on the angle of incidence is chosen. Rayner (1979) suggested that $C_{\mathrm{D,\,pro}}$ can be approximated by $C_{\mathrm{D,\,min}}$ for hovering animals, but this neglects the enhanced pressure drag contribution to the profile drag that must be expected at the observed large angles of incidence. The angles of incidence were not known in Weis-Fogh's (1973) analysis of hovering, so he estimated the drag coefficient by dividing the calculated mean lift coefficient by a chosen value of $C_{\mathrm{L}}/C_{\mathrm{D}}$. A ratio of 7.5 was used for most insects, based on the measurements of Jensen (1956). The drag coefficient thus obtained included induced drag in addition to profile drag because real wings were used in Jensen's experiments. The drag coefficients are still remarkably low, however, and about the same as the minimum profile drag coefficient predicted by equation (9). This is because of the abnormally low drags measured

by Jensen. Based on the *Tipula* and *Drosophila* polars in figure 2 and an arbitrary allowance for the induced drag contribution, I think $C_{D,\,pro}$ is more likely to be about 0.15–0.2 at *Re* of 1500, increasing to perhaps 0.5 at *Re* around 200. Any estimates of profile drag must be treated very cautiously, though, until measurements are made for wings executing the motions of hovering.

I thank Dr K. E. Machin for imaginative discussions and for reading the manuscript, and the Science and Engineering Research Council for financial support.

References

Bennett, L. 1970 Insect flight: lift and rate of change of incidence. *Science, N.Y.* **167**, 177–179.
Bennett, L. 1977 Clap and fling aerodynamics – an experimental evaluation. *J. exp. Biol.* **69**, 261–272.
Bramwell, A. R. S. 1976 *Helicopter dynamics*. London: Edward Arnold.
Buckholtz, R. H. 1981 Measurements of unsteady periodic forces generated by the blowfly flying in a wind tunnel. *J. exp. Biol.* **90**, 163–173.
Carpenter, P. J. 1958 Lift and profile-drag characteristics of a NACA 0012 aerofoil as derived from measured helicopter-rotor performance. *Tech. Notes natn. advis. Comm. Aeronaut., Wash.* no. 4357.
Chadwick, L. 1940 The wing motion of the dragonfly. *Bull. Brooklyn ent. Soc.* **35**, 109–112.
Clements, R. R. & Maull, D. J. 1975 The representation of sheets of vorticity by discrete vortices. *Prog. Aerospace Sci.* **16**, 129–146.
Cloupeau, M., Devilliers, J. F. & Devezeaux, D. 1979 Direct measurements of instantaneous lift in desert locust; comparison with Jensen's experiments on detached wings. *J. exp. Biol.* **80**, 1–15.
Crabtree, L. F. 1959 The formation of regions of separated flow on wing surfaces. *Rep. Memo. aeronaut. Res. Comm.* (*Coun.*) no. 3122.
Duncan, W. J., Thom, A. S. & Young, A. D. 1970 *Mechanics of fluids*. London: Edward Arnold.
Edwards, R. H. & Cheng, H. K. 1982 The separation vortex in the Weis-Fogh circulation–generation mechanism. *J. Fluid Mech.* **120**, 463–473.
Ellington, C. P. 1975 Non-steady-state aerodynamics of the flight of *Encarsia formosa*. In *Swimming and flying in Nature* (ed. T. Y. Wu, C. J. Brokaw & C. Brennen), vol. 2, pp. 783–796. New York: Plenum Press.
Ellington, C. P. 1980 Vortices and hovering flight. In *Instationäre Effekte an schwingenden Tierflügeln*. (ed. W. Nachtigall), pp. 64–101. Wiesbaden: Franz Steiner.
Farren, W. S. 1935 The reaction on a wing whose angle of incidence is changing rapidly. *Rep. Memo. aeronaut. Res. Comm.* (*Coun.*) no. 1648.
Francis, R. H. & Cohen, J. 1933 The flow near a wing which starts suddenly from rest and then stalls. *Rep. Memo. aeronaut. Res. Comm.* (*Coun.*) no. 1561.
Fung, Y. C. 1969 *An introduction to the theory of aeroelasticity*. New York: Dover.
Furber, S. B. & Ffowcs Williams, J. E. 1979 Is the Weis-Fogh principle exploitable in turbomachinery? *J. Fluid Mech.* **94**, 519–540.
Glauert, H. 1929 The force and moment on an oscillating aerofoil. *Rep. Memo. aeronaut. Res. Comm.* (*Coun.*) no. 1242.
Holst, E. von & Küchemann, D. 1941 Biologische und aerodynamische Probleme des Tierfluges. *Naturwissenschaften* **29**, 348–362.
Jensen, M. 1956 Biology and physics of locust flight. III. The aerodynamics of locust flight. *Phil. Trans. R. Soc. Lond.* B **239**, 511–552.
Kármán, T. von & Burgers, J. M. 1935 General aerodynamic theory – perfect fluids. In *Aerodynamic theory* (ed. W. Durand), vol. 2, Div. E. Berlin: Springer.
Kármán, T. von & Sears, W. R. 1938 Airfoil theory for nonuniform motion. *J. aeronaut. Sci.* **5**, 379–390.
Katz, J. 1981 A discrete vortex method for the non-steady separated flow over an airfoil. *J. Fluid Mech.* **102**, 315–328.
Kiya, M. & Arie, M. 1977 A contribution to an inviscid vortex-shedding model for an inclined flat plate in uniform flow. *J. Fluid Mech.* **82**, 223–240.
Kramer, M. 1932 Die Zunahme des Maximalauftriebes von Tragflügeln bei plötzlicher Anstellwinkelvergrösserung (Böeneffekt). *Z. Flugtech. Motorluftschiff.* **23**, 185–189.
Küssner, H. G. 1941 General airfoil theory. *Tech. Memo. natn. advis. Comm. Aeronaut., Wash.* no. 979.
Lighthill, M. J. 1973 On the Weis-Fogh mechanism of lift generation. *J. Fluid Mech.* **60**, 1–17.
Lighthill, M. J. 1977 Introduction to the scaling of aerial locomotion. In *Scale effects in animal locomotion* (ed. T. J. Pedley), pp. 365–404. London: Academic Press.
Maresca, C., Favier, D. & Rebont, J. 1979 Experiments on an aerofoil at high angle of incidence in longitudinal oscillations. *J. Fluid Mech.* **92**, 671–690.

PHILOSOPHICAL TRANSACTIONS OF THE ROYAL SOCIETY B BIOLOGICAL SCIENCES

Maxworthy, T. 1979 Experiments on the Weis-Fogh mechanism of lift generation by insects in hovering flight. Part 1. Dynamics of the 'fling'. *J. Fluid Mech.* **93**, 47–63.
Maxworthy, T. 1981 The fluid dynamics of insect flight. *A. Rev. Fluid Mech.* **13**, 329–350.
McCroskey, W. J. 1982 Unsteady airfoils. *A. Rev. Fluid Mech.* **14**, 285–311.
McCullough, G. B. & Gault, D. E. 1951 Examples of three representative types of airfoil-section stall at low speed. *Tech. Notes natn. advis. Comm. Aeronaut., Wash.* no. 2502.
Mises, R. von 1959 *Theory of flight.* New York: Dover.
Möllenstädt, W. 1980 Einige Grundzüge der instationären Aerodynamik harmonisch schwingender Tragflügel in inkompressibler, reibungsfreier Strömung. In *Instationäre Effekte an schwingenden Tierflügeln.* (ed. W. Nachtigall), pp. 9–34. Wiesbaden: Franz Steiner.
Nachtigall, W. 1977 Die aerodynamische Polare des Tipula-Flügels und eine Einrichtung zur halbautomatischen Polarenaufnahme. In *The physiology of movement; biomechanics* (ed. W. Nachtigall), pp. 347–352. Stuttgart: Fischer.
Nachtigall, W. 1979*a* Der Taubenflügel in Gleitflugstellung: Geometrische Kenngrössen der Flügelprofile und Luftkrafterzeugung. *J. Orn., Lpz.* **120**, 30–40.
Nachtigall, W. 1979*b* Rasche Richtungsänderungen und Torsionen schwingender Fliegenflügel und Hypothesen über zugeordnete instationäre Strömungseffekte. *J. comp. Physiol.* **133**, 351–355.
Nachtigall, W. 1981 Der Vorderflügel grosser Heuschrecken als Luftkrafterzeuger. I. Modellmessungen zur aerodynamischen Wirkung untershiedlicher Flügelprofile. *J. comp. Physiol.* **142**, 127–134.
Newman, B. G., Savage, S. B. & Schouella, D. 1977 Model tests on a wing section of an *Aeschna* dragonfly. In *Scale effects in animal locomotion* (ed. T. J. Pedley), pp. 445–477. London: Academic Press.
Norberg, R. Å. 1975 Hovering flight of the dragonfly *Aeschna juncea* L., kinematics and aerodynamics. In *Swimming and flying in Nature* (ed. T. Y. Wu, C. J. Brokaw & C. Brennen), vol. 2, pp. 763–781. New York: Plenum Press.
Norberg, U. M. 1975 Hovering flight of the pied flycatcher (*Ficedula hypoleuca*). In *Swimming and flying in Nature* (ed. T. Y. Wu, C. J. Brokaw & C. Brennen), vol. 2, pp. 869–881. New York: Plenum Press.
Norberg, U. M. 1976 Aerodynamics of hovering flight in the long-eared bat *Plecotus auritus*. *J. exp. Biol.* **65**, 459–470.
Osborne, M. F. M. 1951 Aerodynamics of flapping flight with application to insects. *J. exp. Biol.* **28**, 221–245.
Phlips, P. J., East, R. A. & Pratt, N. H. 1981 An unsteady lifting line theory of flapping wings with application to the forward flight of birds. *J. Fluid Mech.* **112**, 97–125.
Prandtl, L. & Tietjens, O. G. 1957 *Applied hydro- and aeromechanics.* New York: Dover.
Rayner, J. M. V. 1979 A vortex theory of animal flight. Part 1. The vortex wake of a hovering animal. *J. Fluid Mech.* **91**, 697–730.
Rees, C. J. C. 1975 Aerodynamic properties of an insect wing section and a smooth aerofoil compared. *Nature, Lond.* **258**, 141–142.
Rüppell, G. 1977 The course of the upper-side flow on a wing model of the Fulmar (*Fulmaris glacialis*) in slow flight. In *The physiology of movement; biomechanics* (ed. W. Nachtigall), pp. 287–295. Stuttgart: Fischer.
Sarpkaya, T. 1975 An inviscid model of two-dimensional vortex shedding for transient and asymptotically steady separated flow over an inclined plate. *J. Fluid Mech.* **68**, 109–128.
Savage, S. B., Newman, B. G. & Wong, D. T.-M. 1979 The role of vortices and unsteady effects during the hovering flight of dragonflies. *J. exp. Biol.* **83**, 59–77.
Sears, W. R. 1976 Unsteady motion of airfoils with boundary-layer separation. *AIAA Jl* **14**, 216–220.
Tani, I. 1964 Low-speed flows involving bubble separations. *Prog. aeronaut. Sci.* **5**, 70–103.
Theodorsen, T. 1935 General theory of aerodynamic instability and the mechanism of flutter. *NACA tech. Rep.* no. 496.
Thom, A. & Swart, P. 1940 The forces on an aerofoil at very low speeds. *Jl R. aeronaut. Soc.* **44**, 761–770.
Vogel, S. 1967 Flight in *Drosophila*. III. Aerodynamic characteristics of fly wings and wing models. *J. exp. Biol.* **46**, 431–443.
Wagner, H. 1925 Über die Entstehung des dynamischen Auftriebes von Tragflügeln. *Z. angew. Math. Mech.* **5**, 17–35.
Wagner, S. 1980 Einfluss der instationären Strömung auf die Aerodynamik des Hubschrauberrotors. In *Instationäre Effekte an schwingenden Tierflügeln* (ed. W. Nachtigall), pp. 35–59. Wiesbaden: Franz Steiner.
Walker, P. B. 1931 A new instrument for the measurement of fluid motion; with an application to the development of the flow around a wing started impulsively from rest. *Rep. Memo. aeronaut. Res. Coun.* no. 1402.
Weis-Fogh, T. 1972 Energetics of hovering flight in hummingbirds and in Drosophila. *J. exp. Biol.* **56**, 79–104.
Weis-Fogh, T. 1973 Quick estimates of flight fitness in hovering animals, including novel mechanisms for lift production. *J. exp. Biol.* **59**, 169–230.
Williamson, C. & Ellington, C. P. 1984 In preparation.
Withers, P. C. 1979 Aerodynamics and hydrodynamics of the 'hovering' flight of Wilson's storm petrel. *J. exp. Biol.* **80**, 83–91.
Withers, P. C. 1981 An aerodynamic analysis of bird wings as fixed aerofoils. *J. exp. Biol.* **90**, 143–162.

PHILOSOPHICAL TRANSACTIONS OF THE ROYAL SOCIETY B BIOLOGICAL SCIENCES

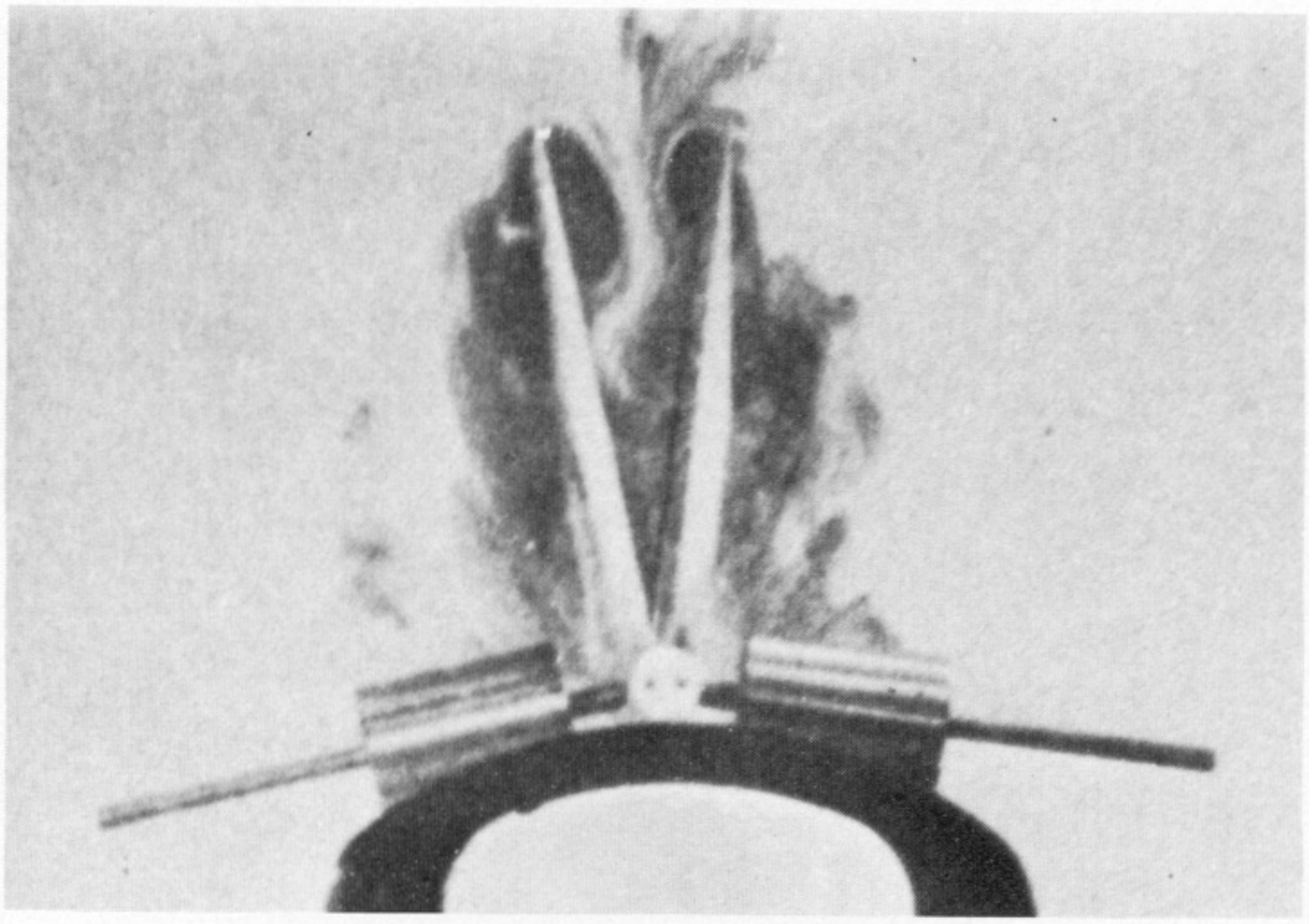

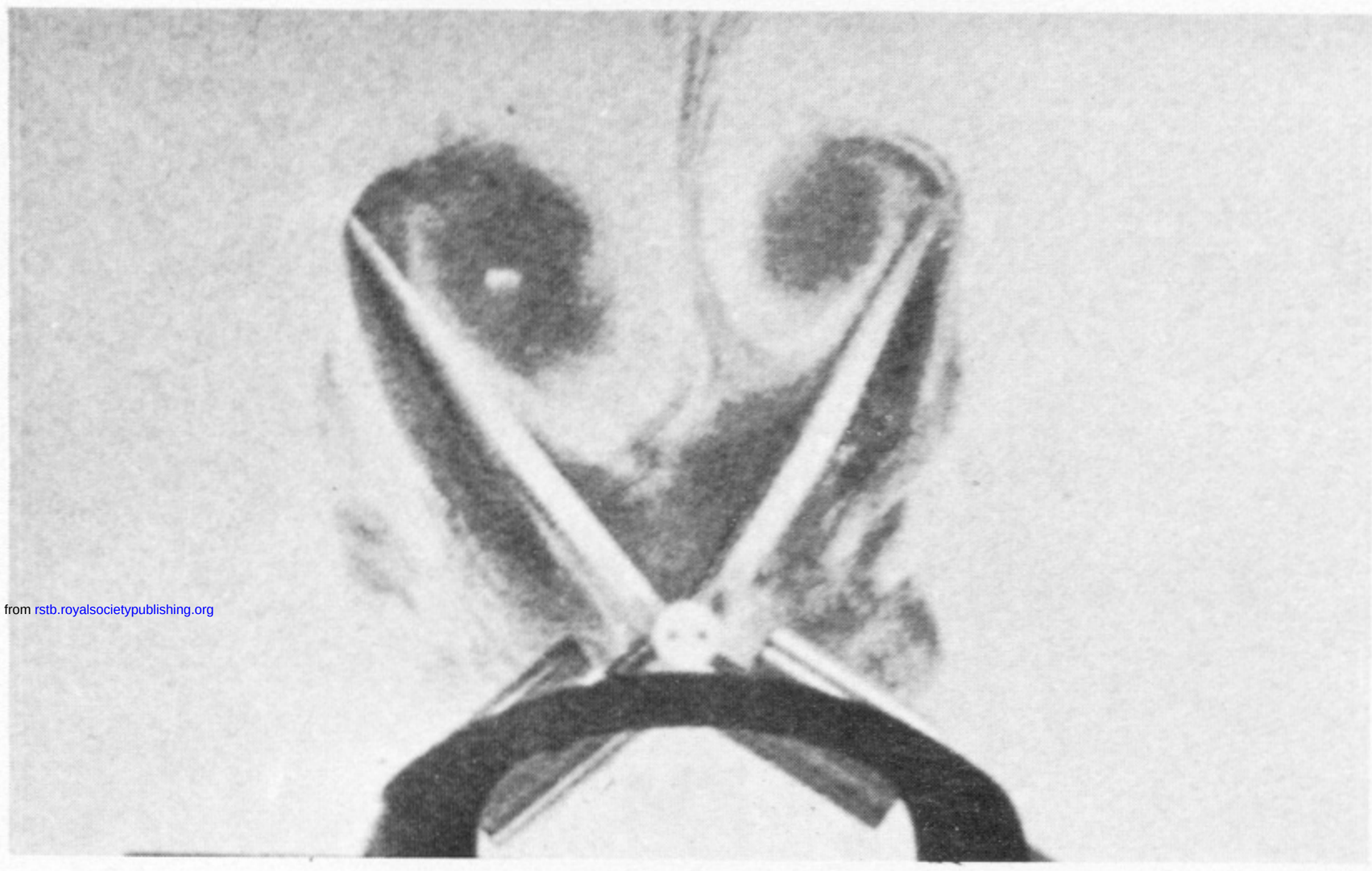

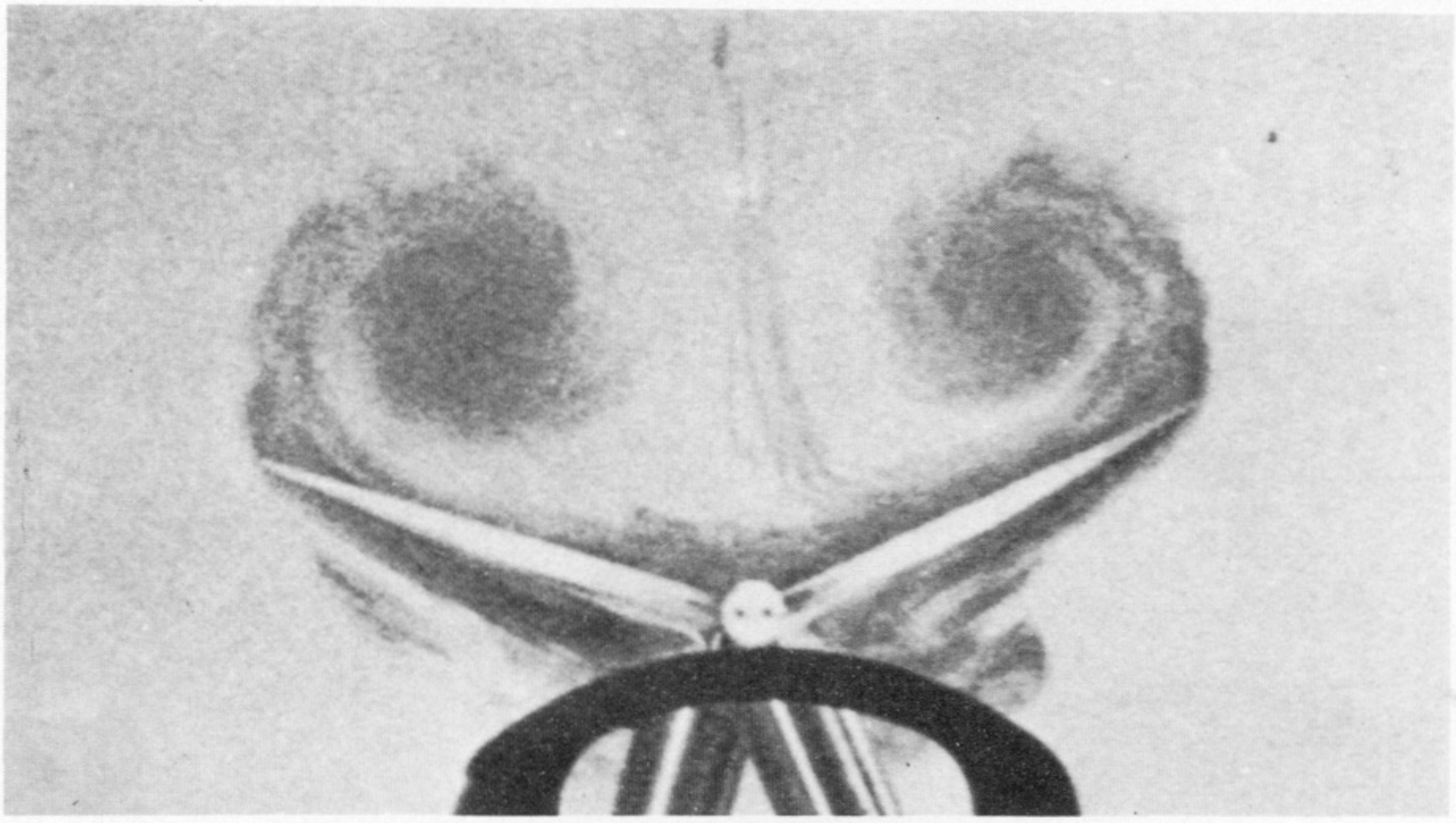

PHILOSOPHICAL TRANSACTIONS OF THE ROYAL SOCIETY B BIOLOGICAL SCIENCES

FIGURE 8. Operation of the fling in a viscous fluid. Vorticity shed from the leading edges rolls up into large leading edge separation bubbles, which contain most of the circulation created by the fling mechanism. From Maxworthy (1979).